

Universidade de Lisboa

Faculdade de Ciências

Departamento de Biologia Animal



**Role of N-Cadherin During
Somitogenesis in the Chick Embryo**

Ana Raquel Marques Jacinto

Mestrado em Biologia Evolutiva e do Desenvolvimento

2010/2011

Universidade de Lisboa

Faculdade de Ciências

Departamento de Biologia Animal



**Role of N-Cadherin During
Somitogenesis in the Chick Embryo**

Ana Raquel Marques Jacinto

Mestrado em Biologia Evolutiva e do Desenvolvimento

**Dissertação orientada por
Dr Gabriel G. Martins**

2010/2011

“Serpenteio, mas não me desvio”

*Carvalho Monteiro, entomólogo
e idealizador da Quinta da Regaleira*

Agradecimentos

Terminada a escrita da minha tese e fazendo uma retrospectiva, apercebo-me do grande número de pessoas que, de uma forma ou de outra, a tornaram possível e às quais não posso deixar de expressar o meu grato reconhecimento.

Assim e em primeiro lugar, ao meu incansável orientador, Dr. Gabriel Martins, que tornou este caminho complicado num “passeio agradável”, partilhando a sua vasta experiência e, ainda assim, permitindo-me cometer os meus erros e resolver os problemas com grande autonomia. Por todo o *brainstorming*, por toda a paciência, por toda a confiança e por toda a sabedoria que me transmitiu, o meu muito obrigado.

Queria também agradecer a todo o grupo de Development and Evolutionary Morphogenesis pelo apoio e boa disposição, pelas conversas científicas e filosóficas, pelos conselhos e pelos puxões de orelhas.

À Prof. Dra. Solveig Thorsteinsdóttir, pelo apoio e pelo entusiasmo com cada pequeno resultado obtido, por ter partilhado ideias e hipóteses.

À Prof. Dra Gabriela Rodrigues, pelo bom humor e conselhos úteis nas culturas.

À Marianne Deries, por me ter permitido experimentar o meu inglês até quase à exaustão, por ter sido tão boa companhia e ter transmitido tanto conhecimento dentro e fora da ciência.

À Raquel Vaz, pelo sorriso fácil e a gargalhada ainda mais fácil. Contigo ao pé, a animação é contínua e a aprendizagem constante.

Ao Pedro Rifés, por me ter ensinado a valiosa lição da diferença entre o estar marcado e o não estar marcado. Espero tê-la aprendido bem e levá-la-ei comigo durante a minha carreira científica.

Ao Luís Marques, por ser como é e por traduzir as músicas mais lamexas para português, pelas conversas sobre *ScienceFiction* e pela boa disposição.

A todos os meus colegas que durante este ano estiveram na mesma situação que eu: Patrícia Almeida, Joana Mateus e André Gonçalves. Este ano não teria tido nem metade da piada se vocês não estivessem lá para desesperar comigo. Por todo o apoio, compreensão, espírito de entreajuda que demonstraram, posso dizer com convicção que os vossos futuros colegas de profissão têm imenso a ganhar ao conhecer-vos e ao trabalharem convosco. Eu sei que ganhei.

À Dona Branca, pelo encorajamento e confiança vindos de quem já viu muitos como nós passarem pelo mesmo.

À malta do C2, por partilharem gargalhadas e conselhos e músicas que faziam doer os ouvidos mas que nos deixavam a pedir por mais. Porque a biologia e a investigação vai para além das fronteiras que são as portas de cada laboratório. A todos os meus amigos de curso que tornaram este ano colorido e cheio de vida. A vocês, Andreia, Margarida, Patrícia, Inês, Catarina, Sofia e Joana, o meu muito obrigado. O vosso apoio foi inestimável, a vossa paciência inesgotável e o vosso humor divinal.

A todas as pessoas que, de uma forma ou de outra, contribuíram para que esta tese chegasse a bom porto. À Chaya Kalcheim por ter cedido os vectores com a versão truncada da N-caderina. Ao Dr. Jiankai Luo e ao seu estudante de doutoramento, Juntag Lin, por toda a disponibilidade e por terem enviado o plasmídeo de Cadherin11. À Dr. Leonor Saúde e à sua estudante de doutoramento Raquel Mendes, por me terem cedido ao sonda de N-cadherin. Mas em especial por me terem recebido no seu laboratório e por todos os conselhos úteis sobre culturas e Técnica de New, conhecimento esse essencial para o bom desenvolvimento desta tese.

Aos meus três pilares. À minha família, que me carregou e aturou. Eu não seria nada sem vocês e a vocês tudo devo. Obrigada por tudo. A vocês, minhas Bananas, porque são praticamente família. Porque vocês são insubstituíveis e valiosas para mim. Que um dia eu vos dê em triplicado tudo o que vocês já me deram. Obrigada por me deixarem partilhar. E a ti... Porque foste um pilar para o bom e para o mau, mas essencialmente para o assim-assim, quando não se estava nem bem nem mal. Por todo os raspanetes e por todo o conhecimento que partilhaste comigo, estou-te grata.

A todos o meu muito obrigado.

Abstract

The first evidence of metamerization in the vertebrate body plan is the segmentation of the paraxial mesoderm into somites which happens early during the embryonic development. The genetics and signalling involved in the process have already been thoroughly studied, and recent works have shed some light in the morphogenetic movements that presomitic mesoderm cells undergo and during somite formation and epithelialisation. In the present work, the role of the adhesion molecule N-cadherin in somitogenesis was studied in more detail. The expression pattern in chick embryo has previously been shown, as well as the common defects caused by the lack of N-cadherin in mouse embryo. Though apparently not fundamental for the somite formation, N-cadherin is important for the correct epithelialization. By electroporating two different truncated versions of the N-cadherin, one without the extracellular domain and another without the intracellular domain, it was visible that the somites formed had different sizes when compared with the control and other phenotypes occurred: fusions and fissions of somites. Preliminary results showed that each domain of the N-cadherin affects differently the medial, rostral and caudal epithelia in terms of number and position of cells, which suggests that both domains mediate cellular events which important for the correct epithelialization and maintenance of the epithelium. Because previous work in chick embryo suggested that the first ten formed somites were more susceptible to the impairment of N-cadherin, so the expression patterns of N-cadherin and cadherin11 were studied for these stages. The hypothesis was that both cadherins would be cooperating in the 10th somite and beyond, so cadherin11 would compensate for the lack of N-cadherin and reduce the effects visible in the first ten somites. This was not confirmed, since cadherin11 only expresses transiently in the somites first ten somites. This work sheds light into the possible role(s) of N-cadherin during early somitogenesis.

Keywords: Somitogenesis, N-cadherin, Cadherin11, Epithelium Assembly, Cell Dynamics

Resumo

Os sómitos são a primeira estrutura metamérica visível aquando do desenvolvimento dos vertebrados, e formam-se aos pares por segmentação da mesoderme paraxial no eixo antero-posterior, um processo ao qual se dá o nome de somitogénese. Para isto, as células mesenquimatosas da mesoderme paraxial têm de fazer uma transição mesênquima-epitélio e posicionar-se no local correcto. Esta transição exige que as células sofram várias modificações na sua morfologia, o que ocorre de uma forma dinâmica. As células na parte média da mesoderme paraxial não segmentada tornam-se progressivamente epiteliais à medida que se aproximam do momento de formarem sómitos. Algumas células mesenquimatosas ligam-se a células já epiteliais e usam-nas para elas mesmas se tornarem epiteliais, um movimento a que se dá o nome de acreção. Este movimento parece ser o principal responsável pela formação do epitélio rostral e caudal. Outros movimentos também ocorrem, culminando num sómito composto por um epitélio de células epiteliais à volta de um centro de células mesenquimatosas, o somitocélio. À medida que o sómito passa pelo processo de maturação, o epitélio ventral dissocia-se no dermamiótomo e no esclerótomo. Estes originam no indivíduo adulto as vertebrae, os discos intervertebrais, as costelas, os músculos esqueléticos e os tendões dos membros. O processo de somitogénese é controlado no tempo, com cada par de sómitos a formar-se num intervalo de tempo específico. No caso do embrião de galinha, cada par de sómitos forma-se com um intervalo de 90 minutos.

Para alguns dos movimentos ocorrerem, as células têm de conter na sua membrana moléculas que lhes permitam estabelecer ligações mais ou menos temporárias com outras células. A estas dá-se o nome de moléculas de adesão celular e podem ser classificadas em quatro grupos: integrinas, imunoglobulinas, selectinas e caderinas. O presente trabalho incidiu sobre as caderinas e sobre o seu papel especificamente na somitogénese. Estas moléculas são glicoproteínas que medeiam uma adesão dependente de cálcio e estão geralmente implicadas no desenvolvimento embrionário, desempenhando vários papéis diferentes como segregação, condensação e rearranjo de células de estruturas em formação. Actuam como dímeros e o domínio extracelular medeia uma adesão homofílica, ou seja, adesão entre duas moléculas iguais. O domínio intracelular, por sua vez, veicula a ligação ao citoesqueleto celular. A N-caderina está presente na parte mais posterior da mesoderme paraxial, junto ao nó de Hensen, e tem uma expressão na parte não segmentada que decresce à medida que se aproxima da parte rostral. Na zona onde se está a dar a formação dos sómitos, a expressão de N-caderina é retomada e aumenta no sómito em formação, depositando-se na parte apical das células que está virada para o centro do sómito. A expressão mantém-se até ao momento de formação do esclerótomo na parte ventral, onde o epitélio se dissocia e as células dispersam. Antes de isto acontecer, a N-caderina é sub-expressa no epitélio ventral, mantendo-se apenas a expressão no dermamiótomo. Estudos passados demonstraram que o *knockout* da N-caderina no embrião de ratinho leva à formação de sómitos com formas irregulares e com epitélios onde as células parecem menos coesas.

No embrião de galinha, estudos feitos com um anticorpo que bloqueia esta molécula originaram também sómitos cujo epitélio apresentava defeitos. Isto sugere que a N-caderina não é essencial para a formação do sómito, mas é importante para sua correcta epitelização do sómitos, o que influencia a forma geral do mesmo.

Um dos objectivos deste trabalho foi o de perceber como é que o epitélio é de facto afectado pela falta da N-caderina. Para isso, embriões de galinha com 24 horas foram electroporados com versões diferentes de construções truncadas de N-caderina: uma cujo domínio intracelular não estava presente (cbr-) e outro cujo domínio extracelular foi também removido (Δ 390). Depois da incubação os embriões foram processados e observados ao microscópio confocal. Ambos os vectores produziram defeitos: no cbr- os embriões tinham sómitos geralmente maiores ao longo do embrião; no Δ 390 os sómitos S11-S14 eram geralmente maiores, enquanto que os sómitos S16-S18 eram mais curtos na medida rostral-caudal. Para ambos os vectores, os sómitos S16-S18 eram mais altos do que os do controlo, sendo que os Δ 390 eram os que apresentavam o valor mais elevado. A seguir, reconstruíram-se sómitos e mediu-se o volume do epitélio e do somitocélio para calcular o rácio mesênquima/epitélio. Isto permitiu determinar se a falta da N-caderina provocava um problema na epitelização inicial do sómito ou não. Os valores preliminares encontrados, para os sómitos mais posteriores, foram inferiores aos valores obtidos para os controlos o que sugere um problema na distribuição das células entre somitocélio e epitélio (mais células no epitélio), e um epitélio menos compacto, traduzindo-se num epitélio maior e reduzindo o rácio. Olhando para a distribuição das células no epitélio e no somitocélio, viu-se que os sómitos tratados com cbr- tinham um epitélio mais desorganizado do que o controlo, com mais núcleos contados e com formas mais arredondados, com mais espaço entre eles, enquanto que o somitocélio continha menos células. Tudo isto parece justificar um rácio menor e a ocorrência de sómitos maiores. No caso dos Δ 390, os sómitos têm um epitélio mais compacto, o que explica o facto de os sómitos serem menos largos, mas também têm um somitocélio com menos células e o sómito é mais espesso dorso-ventralmente, o que explica o rácio menor. Estes resultados sugerem que o domínio intracelular é importante durante a formação do sómito pois parece influenciar significativamente a forma das células e consequentemente a forma dos sómitos, e que o domínio extracelular é também importante para a correcta posição das células no epitélio, uma vez que sem ele o epitélio parece estar mais desorganizado.

Dois outros fenótipos também encontrados foram fissões e fusões de sómitos. Uma fissão corresponde a dois sómitos lado a lado onde deveria estar apenas um, e uma fusão é a junção de dois sómitos pelos epitélios rostral e caudal, com partilha de somitocélio. Estes fenótipos foram encontrados em ambos os tratamentos, mas com frequências diferentes, sendo que as fusões estavam mais associadas Δ 390 e as fissões mais associadas ao cbr-. Como em ambos os casos o que parece estar a falhar são os epitélios rostrais e caudais, tal fenómeno apoia para a ideia de que a falta de um dos componentes da N-caderina perturba a correcta acreção de células para estes epitélios, pelo que estes serão mais frágeis e poderão levar a este tipo de fenótipos. Num dos

embriões filmado a 4D no microscópio confocal, foi visível que o sómito formou-se normalmente mas acabou por se fundir com o sómito da frente quando o epitélio rostral colapsou.

A literatura sugere que os primeiros dez sómitos no embrião de galinha são diferentes dos restantes e mais susceptíveis ao anticorpo contra a N-caderina do que os restantes. Tal poderia ser explicado se esses sómitos fossem mais dependentes de N-caderina, enquanto que os outros contariam com outras caderinas que a compensassem. A caderina11 era uma hipótese, visto que cumpre exactamente este mesmo papel no embrião de ratinho. O padrão de expressão da caderina11 foi estudado para embriões com menos e mais de 10 sómitos e foi apenas encontrado transientemente na parte lateral dos sómitos de embriões com menos de 10 sómitos, não sendo encontrado em mais nenhum ponto na mesoderme paraxial. Estes resultados parecem contradizer a hipótese inicialmente avançada, continuando a deixar sem resposta esta pergunta. Possivelmente, outras moléculas de adesão celular estarão envolvidas neste processo.

Palavras-Chave: Somitogénese, N-caderina, Caderina11, Formação do epitélio, Dinâmica Celular

Index

Abstract.....	I
Resumo	II
I - Introduction.....	1
I.1 Somitogenesis.....	1
I.2 - Cadherins.....	2
I.2.1 N-cadherin.....	4
I.2.2 Cadherin11	5
I.3 Objectives	6
II - Materials and Methods	7
II.1 Embryo Cultures – In ovo and New Techniques	7
II.2 - Embryo treatments.....	7
II.2.1 MNCD-2.....	7
II.2.2 Electroporation of N-cadherin dominant negatives.....	7
II.3 Live-Imaging.....	8
II.4 Immunohistochemistry in whole embryos	9
II.5 In situ hybridization of whole mounts	9
II.6.1 Somite and PSM measurements	10
II.6.2 Processing and analysis of images of N-cadherin protein and mRNA patterns	11
II.6.3 Processing and analysis of time-lapse images (4D) of live embryos	11
III - Results	12
III.2.1 Effect on somite number	14
III.2.2 Effects on somite shape.....	14
III.2.3 Effects on Somite Morphology	17
III.2.4 Effects on Somite Formation.....	21
III.3 Expression Pattern of Cad11 and N-cadherin.....	22
III.3.1 Cad11 mRNA expression pattern.....	23
III.3.2 N-cadherin mRNA Expression Pattern	25
IV - Discussion	28
IV.1 Comparing the Two Techniques: electroporation <i>in New</i> and <i>in ovo</i>	28
IV.1.1 In New vs In Ovo	28

IV.2 Functional Impairment of N-cadherin	29
IV.2.1 Experimental Setup	29
IV.2.2 Different vectors, different phenotypes	30
IV.2.3 Fissions and Fusions	31
IV.3 Expression Pattern of Cad11 and N-cadherin	32
IV.3.1 Cad11 mRNA Expression Pattern	32
IV.3.2 N-cadherin mRNA Expression Pattern	33
V - References	35
VI - Supplementary Material	37

I - Introduction

I.1 Somitogenesis

For the correct formation of tissues and organs during development, cells have to establish and maintain connections in order for them to proliferate, migrate and differentiate. While these morphogenetic processes occur, mechanical forces are generated by the dynamic rearrangements of cell-cell contacts and cytoskeleton, which induce changes in cell shape and motility. This allows the transformation of uniform sheets of cells into specialized and functional three-dimensional structures. As development proceeds, groups of cells remain cohesive while others disassemble their connections in a very dynamic and coordinated way. Epithelial-to-Mesenchymal (EM) interconversion is one of the most common processes and involves rapid modulation of both cell-cell and cell-substratum adhesion (Duband et al., 1987; Aberle et al., 1996; Jamora and Fuchs, 2002).

The presomitic mesoderm (PSM) can be described as a homogeneous rod of mesenchyme located in the caudal region of the embryo. At a very precise moment, a process known as somitogenesis occurs in this structure. Presomitic mesenchymal cells undergo a Mesenchymal-to-Epithelial transition (MET) and are sequentially segmented and transformed into epithelial spheres along the body axis, the somites, in a periodic fashion. They are considered to be the first metameric structures that appear during development. Later on, they undergo a process of maturation and disassemble into the dermomyotome and the sclerotome, originating segmented parts of the adult body such as vertebrae, intervertebral disks, ribs, skeletal bud muscles and limb tendons, imposing a segmentation pattern to the surrounding structures. One of the presomitic cells' intrinsic characteristics is the temporal control. Chick embryo somites form with an interval of 90 minutes between each pair and this seems to be controlled by an intrinsic segmentation program that “informs” PSM cells when to form a somite. This has been known as the molecular clock of the somitogenesis (Duband et al., 1987; Kimura et al., 1995; Stockdale et al., 2000; Freitas et al., 2001; Palmeirim et al., 2008).

Recent studies showed the cell behaviours underlying the somite formation through the live-imaging technology. This revealed that PSM cells undergo several modifications in shape and are more dynamic than previously supposed, showing constant protrusive activity and cell body movements. Somite epithelialization seems to require the organization of these cells in an aster-like form, a process that takes much longer than the 90 minute interval of each new cleft formation. What seems to happen is a series of events that brings the cells from the mesenchymal state to the epithelial somite. The authors saw that there were three types of cells in the somites and PSM. All the cells in the mid PSM are mesenchymal (polygonal shaped cells, motile and with pseudopodia), cells in the centre and lateral part of the rostral PSM were cobblestone shaped, which is considered a signal of somite epithelialisation. As somites form and undergo MET,

cobblestone-shape and mesenchymal cells become fusiform and organize centripetally, with some mesenchymal cells in the core. During this transition, they described three types of movements. In the medial part of the somite (rostral and caudal), PSM cells attach progressively to the basal side of the medial cobblestone-shaped cells and start to elongate and align centripetally. This movement is called “accretion”. In the lateral part of the somite, cells move medially and assemble into an epithelium by “condensation”, becoming fusiform. Cells in the somitocoele (centre of the somite) can also undergo MET and epithelise with the rest of the other cells already epithelialised, in a movement called “egression” (Martins et al., 2009).

During early development, the heterogeneous mesenchymal cell layers with distinct fates are not separated by physical barriers and are continuous from one tissue to another before they segregated into different tissues. One way to do this is for cells with identical markers to cluster together and segregate from others. This can be done with specific adhesiveness of cells, where the main characters would be the adhesion molecules. They can be classified in four groups: integrins, immunoglobulins, selectins and cadherins. For the purpose of this experimental work, we will focus on Cadherins (Kimura et al., 1995; Aberle et al., 1996; Mège et al., 2006).

I.2 - Cadherins

The cadherins superfamily has more than 70 members and allows adhesion through homophilic interactions. Their spatio-temporal expression pattern correlates with morphogenetic events, so they can play different roles during embryonic development such as cell sorting, cell condensation and cell rearrangement. All of these are necessary for tissue to gain integrity and organize cells into a structure with proper form and function, maintaining it throughout life (Kiener and Brenner, 2005). They are glycoproteins and can be subdivided in five gene families: classical cadherins type I (most common), classical cadherins type II, cadherins present in desmosomes, cadherins with very short (or non-present) cytoplasmic domain and protocadherins (Aberle et al., 1996; Miyoshi and Takai, 2008). The mature cadherin contains tandemly arranged cadherin-repeats in the extracellular domain, which forms calcium binding zones that stabilizes the complex and avoids proteolysis (Hirano et al., 1987; Takeichi, 1988).

The first evidences of the adhesive action of these molecules were obtained when cells that do not form tight intercellular connections in monolayer cultures (L cells) were transfected with a full-length E-cadherin cDNA. These cells acquired high Ca^{2+} -dependent aggregating activity and started to form compact colonies (Takeichi, 1988). These experiments also showed that this adhesion happens in an homophilic way rather than interaction with an inherited receptor molecule since only transfected cells were able to adhere – normal cells could not adhere with transfected cells, therefore they did not express any receptor for cadherins. This was further supported by the fact that cadherins typically accumulate at the cell-cell boundary of homotypic cells (Hirano et al., 1987). The extracellular domain has some variability and seems to be the principal responsible for the homophilic recognition between two cadherin molecules. This

recognition is essential for the sorting of heterogeneous cell populations into homotypic subpopulations, like the separation of the neural tube from the neural crest cells (Aberle et al., 1996; Kiener and Brenner, 2005).

The intracellular domain is more conserved, functioning as a binding site for a multitude of molecules, such as catenins, anchoring the structure to the cytoskeleton (Aberle et al., 1996; Derycke and Bracke, 2004). They comprehend two domains, the one where the p120 catenin binds (juxtamembrane domain - JMD) and the one where β -catenin binds (catenin binding domain - CBD). Usually α and β catenins are stabilized by cadherin binding and rapidly degraded upon cadherin-loss. p120ctn is a member of the Armadillo family and have multiple isoforms, not fitting in the classical definition of catenin (Provost and Rimm, 1999; Reynolds and Carnahan, 2004). The roles for p120 and JMD are a little controversial since it has been associated with cadherin clustering and adhesion, translocation, Rho-family GTPases regulation (which are related with cytoskeleton organization and cell motility) and even cadherin turnover (Horikawa and Takeichi, 2001; Kiener and Brenner, 2005). In short, direct p120-E-cad interaction is essential for the cadherin stability and proper epithelial morphology.

Cadherins exist in the form of stable parallel lateral dimers, stabilized by the hydrophobic interaction between the monomers of the extracellular domain (Ivanov et al., 2001). The dimers in one cell establish weak homophilic interactions the dimers in the other cell but as they aggregate in a large number, the effective affinity of the cadherin-cadherin interaction increases. They recruit α -catenin from the cytosol and establish a connection with the actin cytoskeleton (Aberle et al., 1996; Adams and Nelson, 1998; Provost and Rimm, 1999; Jamora and Fuchs, 2002). In the end, they form a structure known as the Adherens Junction (AJ). Recently, this whole model was challenged with a more dynamic hypothesis. Biochemical analysis has shown that α -catenin could not be found in simultaneous interaction with cadherin/ β -catenin complex and actin which undermines the general idea of a highly stable connection. A hypothesis to explain this is to assume that other molecules might be mediating the interaction. Another explanation is that the connection is mediated by many weak and transient interactions that become stronger because there are many cadherins clustered together while still maintaining the ability to easily remodel the connections. Instead of establishing a physical connection between cadherin- β -catenin complex and actin, α -catenin might be acting as a molecular switch that regulates actin dynamics at AJs (Gates and Peifer, 2005; Mège et al., 2006).

Alterations in the expression and/or function of cell-cell adhesion molecules are correlated with major defects in embryonic development (Derycke and Bracke, 2004). In mouse embryos, the lack of E-cadherin and α -catenin induces death at the blastocyst stage due to a failure to form a trophoectodermal epithelium (Jamora and Fuchs, 2002) and perturbation of type I cadherin function can affect somite rotation and muscle differentiation in the *Xenopus* embryo (Giacomello et al., 2002). Loss of E-cadherin is frequently associated with progression of malignancy in tumours, probably because its

loss also affects the Rho-GTPases system (Reynolds and Carnahan, 2004; Kiener and Brenner, 2005).

Instead of “tissue-specific” molecules, each cadherin subclass can be detected in a variety of tissues, showing a unique spatiotemporal pattern throughout the development of the embryo and adult life. This, associated with a tight regulation, allow the use of the same molecules for specific cell adhesions at different positions and different developmental stages (Takeichi, 1988).

I.2.1 N-cadherin

N-cadherin was first identified in 1982 by Grunwald in the chick neural retina (Grunwald et al., 1982). It is a molecule with 130 kDa and belongs to the classical type I. It can induce a motile phenotype when is transfected into epithelial cells, inducing morphology and behaviour changes (Derycke and Bracke 2004). It has also been shown that it can induce invasion and metastasis (Hazan et al., 2000). It is ubiquitously expressed in the neuroepithelium of the developing chicken brain. When blocked in a time of development that corresponds to a massive cellular rearrangement by proliferation and migration, the epithelial structure breaks and the the neuroepithelial tissue loses coherence (Ganzler-Odenthal and Redies, 1998). Also in zebrafish, Rieger et al. (2009) have established that this molecule plays a major role in the migration of the cerebellar granule neurons by interconnecting adhesion, increasing cohesion and allowing the coordination of the migration movements.

The first appearance in development of N-cadherin is during gastrulation when some ectoderm cells are about to invaginate through the primitive streak. These cells initially have N-cadherin and E-cadherin, but while differentiating into mesoderm, they lose the E-cadherin expression – N-cadherin indicates the differentiation into functional mesenchymal cells. It has been shown that N-cadherin mutant embryos initiate gastrulation normally, which suggests that this molecule is not essential in the early processes of mesoderm differentiation and migration (Chuai and Weijer, 2009). The N-cadherin expression accompanies the differentiation of the mesoderm into different tissues in a dynamic way. The mesodermal cells of the paraxial mesoderm organize into a cylindrical epithelial structure with core cells. In this structure, the N-cadherin expression becomes weakly polarized onto the luminal side of the epithelium. As the cylinder segments into U-shaped units through the movements explained earlier, cells increase the expression of N-cadherin in the luminal side of the epithelium. Accordingly, a 3D reconstruction of the apical N-cadherin reveals a “3D adhesion basket” that is opened rostrally and laterally while is still forming (Martins et al., 2009). When the epithelium of the forming somite closes, N-cadherin expression becomes homogenous in the whole somite. The N-cadherin-deficient mesoderm in mice embryo still condenses and forms somites but they are irregularly shaped and cells appear less cohesive. This phenotype is not as severe as the disassociation that occurs in chick pre-somitic mesoderm explants cultured in the presence of a blocking antibody (Duband et al., 1987). The fact that mouse embryo somites are still present indicates that N-

cadherin is not essential for their formation, though it seems very important for the correct organization of the epithelium. The same happens in the chick embryo, as it was shown by Linask et al. (1998) in their experiments with MNCD-2 antibody (Duband et al., 1987; Radice et al., 1997; Horikawa et al., 1999; Martins et al., 2009).

Unpublished data has shown that after blocking the chick embryo somitogenesis with the MNCD-2 antibody, the more affected somites could not epithelise in the caudal and rostral parts, the regions where the epithelium seems to be mainly formed by accretion. One hypothesis is that, with N-cadherin impaired, PSM cells fail to undergo accretion to medial cells and therefore cannot complete epithelialisation (Martins et al., 2009). This could happen because cells might require N-cadherin to attach to the epithelial cells already present in the forming somite. This hypothesis has not been tested yet.

As the somite matures, N-cadherin is downregulated where cells will become mesenchymal again and give rise to the sclerotome, and though retained in the dermomyotome, it is reduced in cells which begin migrating. The cells from the myotome continue to express N-cadherin until the differentiation of skeletal muscles occurs, playing a role in later phases of myotome development (Duband et al., 1987; Takeichi, 1988; Cinnamon et al., 2006).

I.2.2 Cadherin11

Cadherin11 typically confers specific cell-cell adhesiveness on cells and interacts with catenins. It is mainly expressed in mesenchymal cells and its expression pattern is associated with many morphogenetic events. During mouse embryo development, it appears during the formation of new somites and in the progress zone in the early limb buds. This expression pattern is different from those of any other cadherins which suggests it plays a particular morphogenetic role in the control of mesenchymal cell-cell associations and development. During mouse somitogenesis, cad11 expression only starts when somitogenesis begins, thus suggesting a role during this process. When the somite matures and originates the dermomyotome and the sclerotome, only the later maintains the expression of cad11, a pattern complementary to that of N-cadherin. This suggests that the switching of these two cadherins might be correlated with cell segregation processes (Kimura et al., 1995). Cad11 is constitutively expressed in the osteoblast lineage when in cell culture and works in cell sorting, alignment and separation throughout differentiation. It was also showed a role for this molecule on synovial cells during their morphogenetic movement into the synovial lining architecture. When expressed on L-cells, they became connected with one another, condensed and formed aggregates. When in higher densities, Cad11-positive cells formed continuous sheets, a phenotype quite different from the N-cadherin-positive cells that formed spherical aggregates (Kii et al., 2004; Kiener and Brenner, 2005).

Although usually cadherins are associated with tight cell adhesion, the strong presence of cad11 on mesenchymal cells seems to suggest otherwise. Since these cells are loosely associated between them, either they have a mechanism to maintain this loose

association even in the presence of cad11, or cad11 has specific properties that confer weak adhesiveness on cells. This fact could be working with the “community effect” phenomenon, where embryonic cells establish mutual communications to maintain their differentiation fates (Kimura et al., 1995).

It seems that cad11 cooperates with N-cadherin during somite formation and maintenance in the mouse embryo, since double knockout for the two proteins produced a more dramatic phenotype. However, the role of cad11 seems relatively minor, since somites were fairly normal in the cad11 mutant mice (Horikawa et al., 1999). It was proposed that cad11 could compensate for the lack of N-cadherin in the mutant embryos, allowing the maintenance of the structure (Radice et al., 1997). There is also evidence that the first ten pairs of somites in chick are different from the remaining somites, not only morphologically but also in the way in which they are formed. For example, the first somites seem to be more affected with the blockage of N-cadherin (Linask et al., 1998). One hypothesis to explain this is that N-cadherin is the only cadherin expressed in the formation of the first somites, while the formation of the remaining somites is dependent of N-cadherin and cad11, which would act synergistically to facilitate morphogenetic movements during somite epithelium assembly. This could explain why the N-cadherin knockout produces fewer defects and why blocking of N-cadherin via antibodies does not produce consistent results after the formation of the first ten somites (Linask et al., 1998); Martins, Amândio & Jacinto, unpublished observations). This hypothesis has not been tested yet.

I.3 Objectives

One of the objectives of this study was to characterize the pattern of expression of N-cadherin and cadherin-11 in early somitogenesis of chick embryos (Luo et al., 2007)), and determine how, when and which cadherins are expressed in the first ten, versus the next ten somites. The other objective was to better understand the defects produced by the impairment of N-cadherin function on somite epithelium assembly, determining which morphogenetic movements are affected and what is the fate of mesodermal cells whose N-cadherin function has been compromised. To do this, I used live-imaging and 3D image analysis of chick embryos electroporated with a PCAGGS-GFP vector and application of N-Cadherin blocking antibodies (Linask et al., 1998) and with two different truncated N-Cad-YFP constructs (Cinnamon et al., 2006).

II - Materials and Methods

II.1 Embryo Cultures – In ovo and New Techniques

Fertilized chicken eggs were incubated at 38°C with saturated humidity for 24 hours. A window was opened in the shell and a portion of albumen was retrieved and stored for posterior use. The exposed embryos were further treated in two ways: electroporation *in ovo* (as described in II.2.2.2) and culture *in New*. For embryos treated with the *New* culture technique, the whole egg yolk was transferred to a bowl with sterile Phosphate Buffered Saline (PBS 1x). Residues of albumen were removed with a glass pipette and the yolk was positioned so the embryo faced upwards. With scissors and thin forceps, the vitelline membrane was cut through the equatorial line and was gently pushed from the yolk, transporting the embryo with it. The vitelline membrane and the embryo were transported to a glass petri dish and a clean glass ring washed in PBS 1x was placed on top of the vitelline membrane, with the embryo placed on the center of a glass ring. With thin forceps, the vitelline membrane was placed on top the rim and the excess trimmed. The embryo and membrane were washed with fresh PBS 1x and all the PBS was removed from inside the ring. Then, the ring was transferred to a plastic petri dish filled with 2-3 mL of thin albumen (New, 1955; Scaal et al., 2004; Voiculescu et al., 2008). The embryos were then staged according to Hamburger and Hammlton (Hamburger and Hamilton, 1992); the stages used varied between HH4 and HH6.

II.2 - Embryo treatments

II.2.1 MNCD-2

Embryos were bathed with 1,5-2uL of MNCD-2 (D.S.H.B.) and incubated for 24-28h. For the control embryos, the same amount of PBS 1x and time of incubation were used.

II.2.2 Electroporation of N-cadherin dominant negatives

The vectors used were gently given by Dr Kaya Calcheim (Cinnamon et al., 2006) and were: N-cadherin-YFP with an actin promoter and the dominant negatives Δ 390-YFP (N-cadherin construct without the extracellular domain) and CBR-YFP (without the intracellular domain). These constructs were used to transform bacteria from which we later isolated (using a Genomed midi-prep system) the three vectors with final concentrations of 2,48 ug/mL, 2,73 ug/mL and 2,08 ug/mL, respectively. Because in our confocal system we could not detect YFP efficiently, in some cases a GFP vector (Momose et al., 1999; as in Martins et al 2009) was co-electroporeated (1,14 ug/mL; used as a 1:1 dilution of both plasmids) to facilitate identification of electroporated cells; this same plasmid was used to film control embryos.

The electroporation was done using a custom made electroporator programmed to apply 9v pulses with the duration of 25ms with an interval of 333ms. A total of 35 pulses were applied to each embryo for each culture conditions.

II.2.2.1 Electroporation *in New*

The ring was transferred to an electroporation chamber filled with HBSS supplemented with 1000U/mL of Pen/Strep (Invitrogen) and the embryo was placed on top of a platinum plate which served as a negative electrode. A thin needle was used to inject the DNA constructs by piercing through the blastoderm until it reached the dorsal side of the embryo, below the Hensen's Node and according to the fate map of Psychoyos & Stern (Psychoyos and Stern, 1996). A platinum (positive) electrode was then placed above the embryo without touching it and electric pulses were applied. After that, the HBSS was removed from inside the ring and the embryo was placed again on the petri dish with albumen and incubated to the desired stage.

II.2.2.2 Electroporation *in ovo*

Exposed embryos at stages HH4-7 were used for electroporation *in ovo*; 2uL of Fast Green FCF (Sigma) 1:500 was applied to the top of the embryo to improve contrast and more reliably stage embryos. A Tungsten sharpened wire pierced through the *area opaca* and served as a positive electrode. The vitelline membrane on top of the embryo was pierced with the glass-capillary and the DNA was injected on the dorsal side of the embryo to fully cover the Hensen's node and primitive streak. The negative electrode was then positioned along the primitive streak at the anterior-most end which is the presumptive paraxial mesoderm territory (Psychoyos et al., 1996), and electric pulses were applied. Then, the electrodes were removed, the embryo was washed with HBSS, the egg was re-sealed with tape and incubated for the desired time (Momose et al., 1999; Scaal et al., 2004).

II.3 Live-Imaging

Some embryos were used for live-imaging with a confocal microscope. The expression of constructs was first assessed using a ZEISS Lumar fluorescence stereoscope, and the selected embryos were transferred to a glass petri dish with PBS 1x upon removal from the the "New" ring and cleaning. Then, the embryo was placed on top of a sterilized 0,4um pore size transwell-collagen-coated membrane (Costar, Life Sciences) with the ventral side facing down and with the vitelline membrane covering the dorsal side to maintain moisture. The excess of liquid was removed with a thin glass pipette and the filter was transferred to a 200uL of culture medium (Medium DMEM 199 [Sigma] supplemented with 5% of Fetal Bovine Serum (Invitrogen), 10% of Chick Serum (Invitrogen) and 1:100 of Pen/Strep (Invitrogen) on a custom-made imaging chamber which consisted of a plastic petri dish with a glass bottom and a larger outer chamber filled with autoclaved water. This apparatus was placed on a Leica SPE confocal microscope pre-heated to 38°C and maintained at physiological conditions throughout the filming period. Stacks with 20-30 optical slices were acquired using a 20x 0.7NA

(dry) lens and with an interval of 6 minutes between each time point for a total duration of at least 6 hours. In some cases, the 63x (water) lens was used, but since it has a low working distance, it only captured in a stack the first layers of cells in the embryo, not even reaching the middle plane.

II.4 Immunohistochemistry in whole embryos

Embryos treated with *mncd2* or electroporated with dominant negative constructs and not processed for live-imaging were seen and photographed on ZEISS Lumar and then collected either from the *News* or from *in ovo*. These embryos were immediately fixed with PFA 4%, at 4°C overnight (ON), and then washed 3x15min in PBS, permeabilized for 2 hours in 0,5% TritonX-100, trimmed for head and excess of blastoderm and staged again. Then, embryos were incubated in primary antibody anti-N-cadherin (BD) 1:100 either ON at 4°C or at RT for 8h. They were washed 3x15min to remove antibody remnants and placed in Goat anti-mouse secondary antibody Alexa 488 (Mol. Probes) 1:1000 with RNase 1:50 and ToPro3 (Mol. Probes) 1:500, for the same period of incubation. In some cases embryos were also counter-stained with Alexa-Fluor 568 Phalloidin (Mol. Probes), while in other cases the embryos were stained simply with Alexa-Fluor 488 Phalloidin (Mol. Probes) + Topro3, as described. After the last washes, embryos were slowly dehydrated in a series of H₂O:Methanol (VWR) (or isopropanol (Merck, ref: 603-117-00-0) for embryos stained with Phalloidin) as in Martins et al. (2009) and stored at -20°C for later processing. Before imaging, embryos were diaphanised by replacing the alcohol with Methylsalicylate (Merck) and each embryo was then mounted between two #0 coverslips and sealed with paraffin. Images were acquired on a Confocal Leica SPE system with a 10x 0.3NA, 20x 0.7NA or 40x 1.15NA lenses. In images of embryos acquired with dry lenses (10x and 20x), the optical slice thickness was corrected by x1.54 (refractive index of methylsalicylate) to compensate for Z-axis distortions caused by mismatched refractive indices. Images obtained with the oil-immersion lens (40x) did not require corrections.

II.5 In situ hybridization of whole mounts

Embryos were selected from stages HH7 to HH13 and fixed ON at 4°C in WISH (Formaldehyde at 37%, 0,5M pH 8 EGTA, NaOH 5M and PBS supplemented with Ca⁺⁺ and Mg⁺⁺) as in Henrique et al. (1995). Then they were washed in PBT (PBS+Tween 20 1%), dehydrated in a crescent series of methanol and stored at -20°C in Methanol 100% until further processing.

Plasmids with the sequences for Cadherin11 (kind gift of Dr Jiankai Luo; Luo et al., 2007) and N-cadherin (kind gift of Leonor Saúde; produced by Raquel Mendes) were used to produce RNA probes labeled with Digoxigenin based on a protocol from Sérgio Simões. In some embryos I used the anti-digoxigenin-AP antibody with BM Purple AP substrate (Roche) and the embryos were observed and photographed *in toto* with the Lumar Stereoscope coupled with a CASIO EX-F1 digital camera. Then, these embryos were embedded in 0.12M phosphate buffer with increasing concentrations of sucrose (as

in Bajanca et al., 2004) and stored at -80°C until they were sectioned on a Bright Clinicut 60 Cryostat and collected on *SuperFrost* Ultra Plus microscope slides. Transversal sections with 14µm in thickness and sagittal sections with 16µm were obtained. These sections were observed on the Olympus BX60 with an Olympus DP50 digital camera with the objectives 20x 0.7NA and 40x 1.0NA.

Other embryos were processed for development with the Fast-red (Roche) chromogen which is also fluorescent (Roche) following a protocol for fish and adapted for chick embryo (Welten et al., 2006). These embryos were then imaged using the confocal microscope; since dehydration with organic solvents causes the loss of the Fast-red chromogen the embryos were slightly diaphanised with glycerol. I obtained z-stacks throughout all full thickness of the somites and PSM, using the same lenses used for immuno-stained embryos. Because the refractive index of glycerol is different from that of air or oil, the optical slices of images collected with dry lenses (10x or 20x) were adjusted by x1.46, while the images obtained with the oil immersion lens (40x) by x0.96, to compensate Z-axis distortions due to refractive index mismatches.

II.6 Image Analysis and Statistics

II.6.1 Somite and PSM measurements

Images from confocal were first processed in Fiji software to increase brightness and contrast, and the following measurements were obtained:

- Somite length and width: major diameters along the AP and ML axii, respectively (Fig.1 “l” and “w”)
- PSM length and width; linear distance between the posterior edge of the last somite formed and the level of Hensen’s node (see Fig.1). The width of the PSM was measured at three different levels, one at the first somitomer, other at the node level and other in a middle distance between these two.

For each embryo we obtained these measurements on both sides and scored them as separate entries in a data table. The final analysis includes measurements of a total of 14 control embryos, 17 *mncd2*, 20 *d390* and 6 CBR-. From each embryo I measured the total number of visible somites, which varied from a minimum of 18 to a maximum of 36 somites per embryo (left and right somites).



Fig. 1 Schematics of the 2D measurements made in the embryos obtained from culture.

To count the cells that were found in somites of $\Delta 390$ treated embryos, four were chosen and 3D reconstructed using the Amira 5.3.3 software. Then cells outside the somite were counted and this process was repeated for eight somites per embryo.

For the study of tissue organization in somites of control *vs.* treated embryos, the confocal Z-stacks were first 3D reconstructed using the Amira v5.3.3 software (Visage Imaging Inc.), and then manually contoured on each optical slice for estimation of epithelial and somitocoelic volumes. This allowed us to surface-render groups of somites (as in Fig.11B&D), with which we also obtained somites thickness along the dorsal-ventral axis. Using the Amira software I also reconstructed an “equatorial” slice (ie, a virtual coronal slice exactly through the middle of each somite), in which lines of 25um were drawn in medial, rostral and caudal epithelia and a line of 20um in the somitocoel and the number of cells intersected by these lines provided an estimate the level of cell compaction on the medial epithelial wall and in the somitocoel. A total of 12 somites were analyzed for each treatment.

II.6.2 Processing and analysis of images of N-cadherin protein and mRNA patterns

The *in toto* images of the embryos developed with BMPurple were processed on the Fiji software where linear contrast and brightness adjustments were done. The sections from the cryostat were also processed with Fiji where each channel was correctly adjusted to produce a white background and brightness and contrast were adjusted.

The images of embryos developed with Fast-red and imaged with the confocal were processed in Fiji and the 3D reconstruction of the expression patterns was achieved in the Amira software, with the broader pattern reconstructed with the 10x stacks and the details obtained from the 40x stacks. Using the Amira software I also obtained plots for the N-cadherin content along the anterior-posterior axis by drawing a “probe” line through the paraxial mesoderm which measured the average pixel intensity in a neighborhood of 40 pixels (see Fig.17H). This analysis was done in images of immunostained embryos (N-cad staining) and in *in situ* hybridization treated embryos (N-cadherin mRNA). One example of the typical pattern for each stage is presented in Figs.17H.

II.6.3 Processing and analysis of time-lapse images (4D) of live embryos

4D sequences of confocal images were also first processed with the Fiji software, where the following contrast adjustments were obtained: gamma increase, thresholding and Gaussian blurring. Also, the 3D natural drift of the embryos was corrected.

III - Results

III.1 Comparing Two Techniques: electroporation *in New* and *in ovo*

For this experimental work, electroporation was performed according to two different culture conditions: *in ovo* (Momose et al 1999) and in “*New*” (New, 1955). For each technique we assessed the survival rate (how many embryos survived electroporation), the efficiency (how many presented fluorescence after incubation) and the accuracy (how many presented fluorescence in the correct place). The results are presented in the Table I for both culture methods. I noticed that as my skills developed, I achieved satisfactory results with both techniques, with survival rates nearing 90% for both. As for the efficiency, *in ovo* electroporation resulted in a higher frequency of embryos with fluorescence, possibly because during electroporation in the *New* Technique the embryos lie submerged in saline, where the vector can dilute. Also, the embryo faces ventral side up and the micro-injection needle has to perforate the blastoderm to be positioned in the correct place. *In ovo*, the dorsal side of the embryo faces upwards and the vector is injected through the vitelline membrane directly in the paraxial mesoderm precursors, so there is less chance for dilution, allowing a more precise electroporation (Fig.2A). Nevertheless, the process occasionally induces damages in the embryo, such as holes or “scars” when applying the electric field. The efficiency varied somewhat among the different vectors, despite the fact that all had comparable concentrations. For example, the cbr- vector was only successfully electroporated *in ovo*, with poor results when electroporated in *New*. On the other hand, only 17% of the cases presented Ncad-YFP when electroporated *in ovo* and expression levels were typically unsatisfactory.

Tables I and II Concentrations of the different vectors used in this experimental work and survival rates, efficiencies and accuracies for each technique and vector, as well as the average time needed for handling and electroporating embryos for each technique.

	[vector] (ug/mL)	Survival Rate (%)	Efficiency (%)	Accuracy (%)	
<i>In New</i>					
	GFP 1,14	88,0	62,1	44,0	
	Ncad-YFP 2,48	87,5	70,1	50,0	
	Δ390 2,73	87,5	38,1	31,3	
	cbr- 2,08	90,0	75,0	40,7	
		85,7	50,0	33,3	
<i>In Ovo</i>					
	GFP 1,14	88,8	80,4	49,4	
	Ncad-YFP 2,48	90,2	88,3	50,0	
	Δ390 2,73	88,5	17,4	25,0	
	cbr- 2,08	94,7	91,7	45,5	
		78,4	86,2	56,0	

	Handling + Electroporation (minutes)
<i>In New</i>	<10min (6-8min) + 3-4min
<i>In ovo</i>	3-5min

In terms of accuracy, the values are usually higher for *in ovo* electroporations, but we cannot rule out an effect due to the different electrodes used for each method. In *New* culture, a pre-assembled chamber with platinum plate electrodes was used, whereas in the *in ovo* culture, sharp tungsten electrodes were used (as in Martins et al., 2009). In the *in ovo* procedure, the process of opening the egg, identifying the stage of the

embryo, correctly position the positive electrode, perforating the vitelline membrane and injecting the vector in the correct place and electroporate with the negative electrode, is fairly quick with practice (between 3-5 minutes, if no major problem with correctly positioning or staging the embryo occurs). In the *New* technique, the embryo is retrieved from inside the egg and cultured *ex ovo*; the process is more time consuming, but with practice I reduced it to <10 min per egg (TableII). Since all embryos are kept at room temperatures during the procedures, the development arrests and all embryos are then incubated simultaneously. The process of electroporation *per se* is quite fast (between 3-5 minutes). The embryo in the *New* Technique is usually quite visible and it can be easily cleaned of yolk remnants, which facilitates further experiments such as delivery of drugs or live-imaging (Fig.2B).

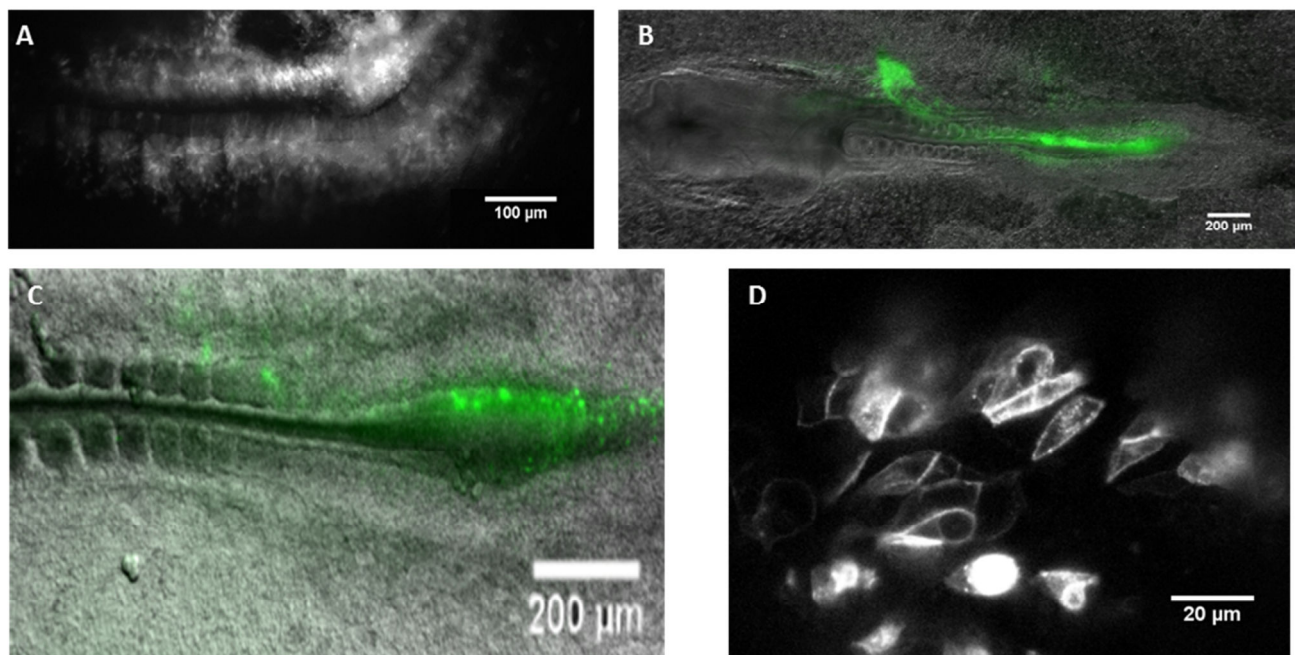


Fig.2 Typical result of GFP electroporation *in ovo* (A) and *in New* (B) and of Ncad-YFP *in New* (C), with a detail of showing the expression on the membrane. Anterior part to the left and posterior part to the right. D is a detail of Ncad-YFP expressing in the cell membrane; this image was obtained with the 63x 1.15W lens, which provided higher resolution but limited working distance for long time-lapse movies..

One of the best Ncad-YFP electroporated embryos is presented in Fig.2C, with a detail in D. The expression was normally weak and visible in few cells. Since it produced poor results, and a signal that was too weak to be detected in our confocal microscope during prolonged time-lapse imaging I focused mainly on the two truncated versions of the vector, the $\Delta 390$ and the *cbr-*.

III.2 Functional Impairment of N-cadherin

The two dominant-negative vectors used impair N-cadherin in different ways: the $\Delta 390$ does not possess the extracellular domain of N-cadherin which disturbs the connection between cells, while the *cbr-* does not present the intracellular catenin binding domain, unsettling the connection with the actin cytoskeleton. The *mncd2* antibody has

previously shown to affect somitogenesis by Linask et al. (1998), and was also used for N-cad functional impairment experiments.

III.2.1 Effect on somite number

I first analysed whether treated embryos produced the expected number of somites, which were predictable because the initial stage and the time of culture were known. As shown in the Fig.3A, *cbr-* treated embryos produced on average less one and a half somite, while the control and *mncd2* treated embryos produced the expected number. Interestingly, the tendency of the $\Delta 390$ treated embryos was to produce more somites than expected. Analysis showed a distribution of 12 cases (out of 34) that formed more somites than the expected and 7 cases that formed less (Fig.3B). Embryos that formed less than 5 somites for all treatments were considered as outliers and removed from the analysis. This was the first evidence that the two vectors might affect somitogenesis differently.

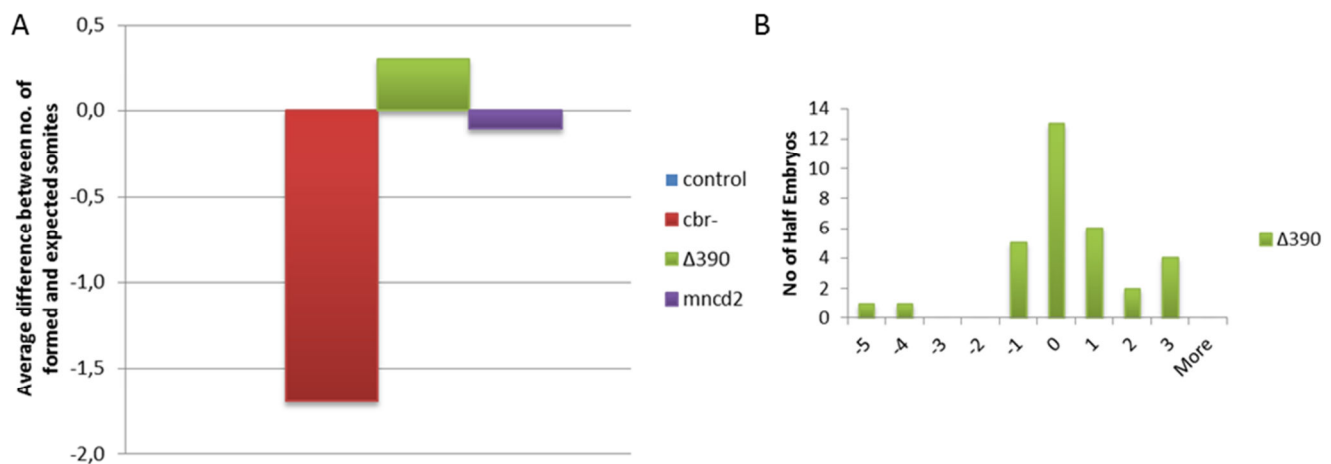


Fig.3 Graphics showing the average difference between the number of formed and the number of expected somites for each treatment (A) and distribution of the number of $\Delta 390$ treated half embryos (left and right for each embryo) that formed less or more or the expected value (B)

III.2.2 Effects on somite shape

To assess the effects on somite formation, I began by measuring the length and width of somites for all embryos; the average values are presented on Fig.4A&B). In control embryos, the most mature somites (S2-S7 in Fig.4A) and the somites recently formed are bigger (S16-S18 in Fig.4A) than somites S9-S15. The largest size of head somites could be explained with the beginning of the formation of sclerotome, and the recently formed by an incomplete cell compaction and epithelial assembly. Though with less variation of values, the width seems to follow the same trend (Fig.4B).

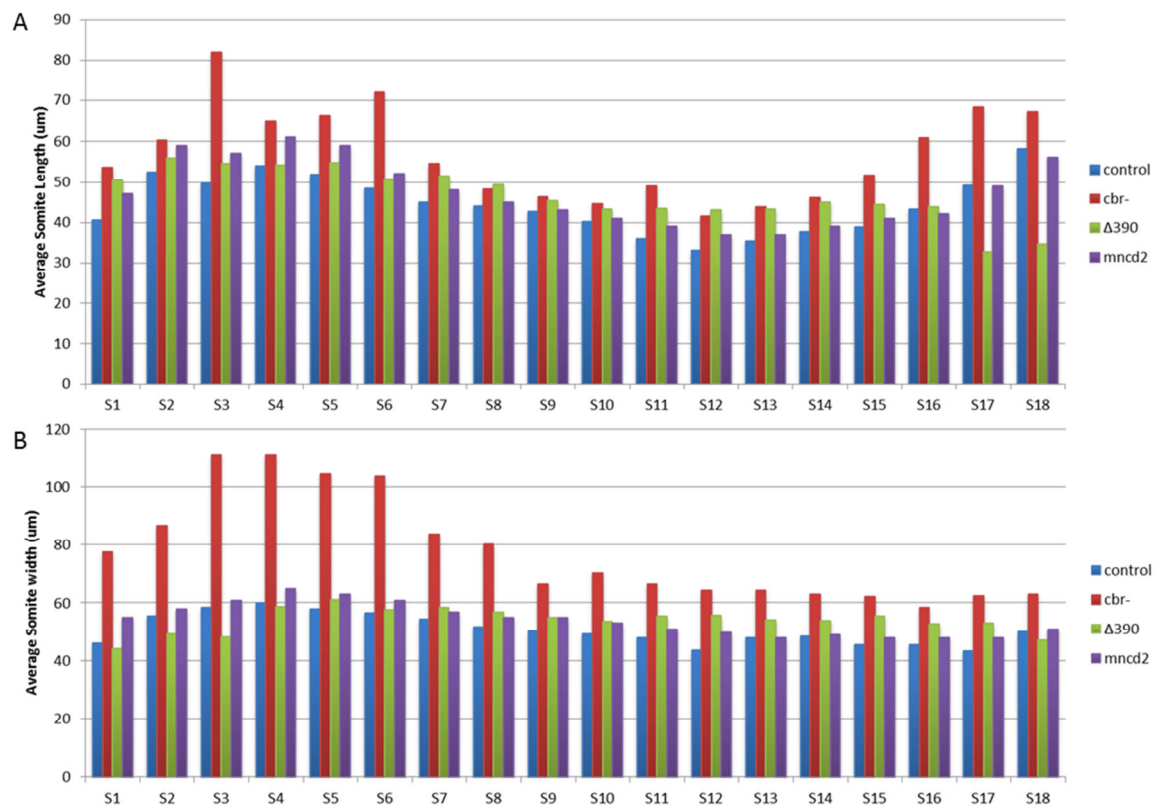


Fig.4 Average somite lengths (A) and widths (B) from first visible somite (S1) to last formed somites (S18). Embryos were electroporated at HH4-6, and cultured for 24-27h before collection, processing, imaging and measurements.

The somites of *mncd2* treated embryos were similar to controls (Fig.4A&B) without signs of the typical defects described by Linask et al. (1998); though they recognized that only a small percentage of cases were in fact affected with this antibody. This suggested that our *mncd2* was not reliably producing effects so the *mncd2*-treated embryos were left out of the rest of the analysis.

In the case of the *cbr-* treated embryos, somite sizes showed a similar pattern, though they were consistently larger, an effect particularly evident in the most recent (S16-S18) and oldest somites formed (S3-S6); furthermore, somites S9-S14 also seemed wider (Fig.4A&B). As for the $\Delta 390$ treated embryos, they followed a pattern similar to controls until somite S12 onwards which were wider and longer but then decreased in length in the last somites formed (S16-S18).

To better understand these differences I next concentrated the analysis on the somite groups which showed more pronounced effects. In the case of the *cbr-* embryos, the measurements were pooled together in the groups S3-S6 and S15-S18 and for the $\Delta 390$ S11-S14 and S17-S18 (Fig.5). Statistical analysis confirmed that somites of *cbr-* embryos were bigger in both measurements (Fig.5A&B, $P < 0.01$), and that $\Delta 390$ -treated somites were significantly different from controls, except for the width of S15-18. In this case, S11-14 are bigger than the controls, while the S15-18 are smaller.

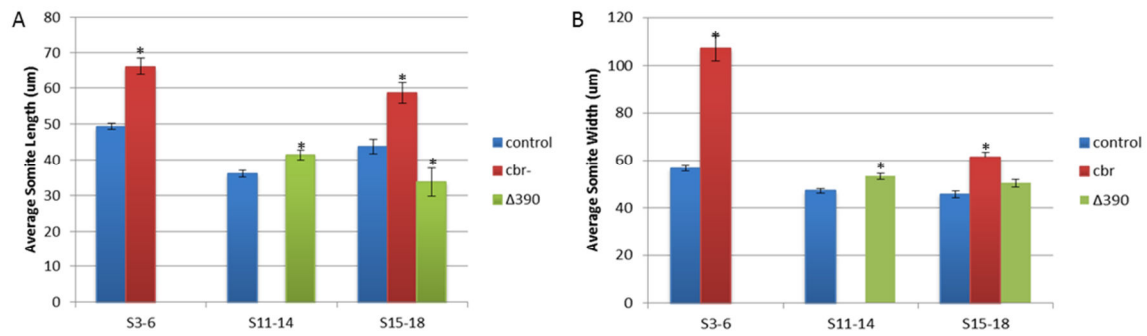


Fig.5 Graphs comparing specific measurements between treated and control embryos, in length (A) and width (B). Bars represent the Standard Error of the Mean (SEM). Statistically significant values are marked with an asterisk (p -value<0,01). Average values of somite length and width on SI&II of Supplementary Materials (Sup.Mat).

In the case of the presomitic mesoderm (PSM), the average values for length and widths are shown in Fig.6A&B. Cbr- treated embryos seem to have longer PSMs while the Δ390 treated embryos have shorter and narrow PSMs than controls. Nonetheless, these differences were not statistically significant except the width of Δ390-treated embryos, which was larger (Fig.6C; P <0,01). However, because we could not use consistent morphologic references when measuring the PSM, these measurements seemed unreliable in determining the existence of effects.

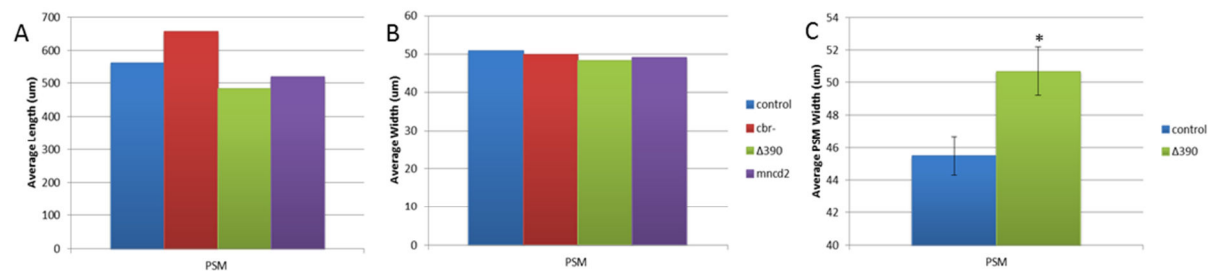


Fig.6 Graphs of the average length (A) and width (B) in microns of the presomitic mesoderm for controls and treated embryos. Significantly differences (asterisk means p -value<0,01) were found between the width of the controls and the Δ390 treated embryos (C). Bars represent the SEM. Average values of PSM width on SIII of Sup.Mat.

The thickness (dorso-ventral diameter) of the somites was measured from 3D reconstructions of whole somites and the average values are shown in Fig.7. An effect is only seen in the recently formed somites (S16-18) for both treatments. Even so, embryos electroporated with Δ390 had the most affected somites for this measure.

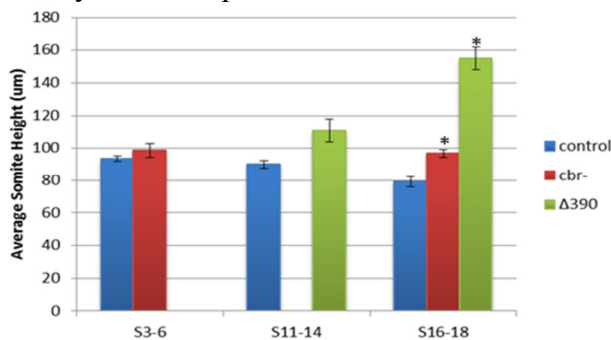


Fig.7 Graph comparing the average height in microns between controls and treated embryos in specific somites. Statistically significant values are marked with an asterisk (p -value<0,01). Bars represent the SEM. Average values on SIV of Sup.Mat.

The differences in size of somites observed suggested impaired cell compaction during somite formation and later dispersal (in preparation for sclerotome formation), and interestingly the “phenotype” was different with both constructs.

III.2.3 Effects on Somite Morphology

Both vectors expressed in somite and PSM cells and fluorescence accumulated on the cell membranes (Fig.8B arrowheads). Though this is expected for cells labelled with *cbr-* (no intracellular domain; Fig.8A), cells without the extracellular domain ($\Delta 390$) epithelialised and attached to other cells, suggesting that other adhesion molecules also contribute for these cells to attach, or that the endogenous expression of WT N-cad in the somites was sufficient to maintain some adhesion functionality (Fig. 8B).

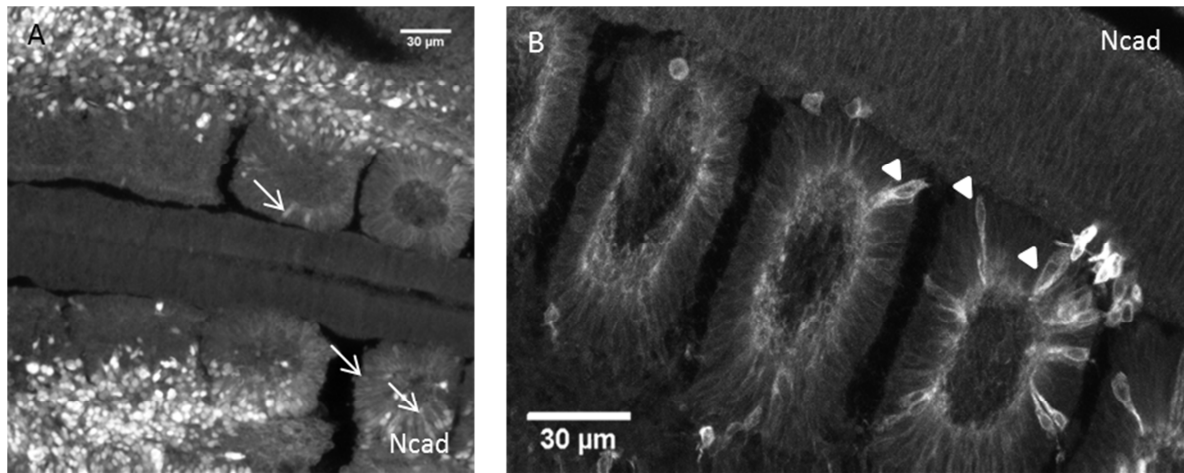


Fig.8 Details of cells labelled with *cbr+gfp* (A, arrows) and with $\Delta 390$ (B, arrowheads). The embryos were processed for immunohistochemistry detection of N-cadherin.

Although most of the somites appear to be normal, there were two other frequent phenotypes: the fission and fusion of somites (Fig.9). Fissions happen when two or more half sized somites appear in the space of one and are characterized by a full epithelium around an independent somitocoel (Fig.9A&B arrows). Normally, the fission occurs medio-laterally separating the somite into two side-by-side halves. Fissions with other orientations were never found in the analysed embryos, though I cannot exclude the possibility that fissions along a medial-lateral plane, separating the somites in rostral and caudal halves, would be a cause for the higher number of somites seen in some cases of $\Delta 390$ treated embryos.

Fusion of somites happen when two somites share a somitocoel, lacking two fully individualized epithelia between them, at least in the middle plane of the somite (Fig.9C). The somitocoel often assumes the shape of a three-dimensional “eight” figure (Fig.9D). This suggests that the intersomitic cleft and the adjacent rostral and caudal epithelial walls collapsed and the medial and lateral walls of the fused somites became contiguous.

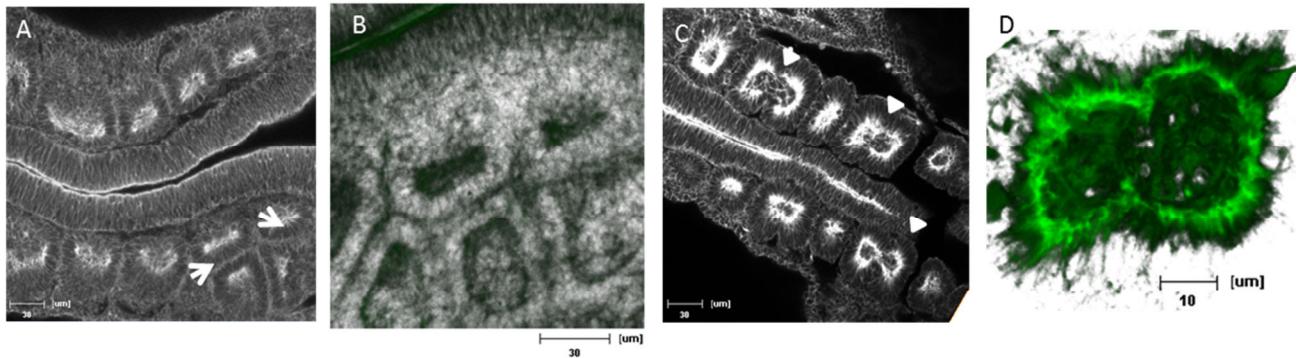


Fig.9 Details of fissions (A and B) and fusions (C and D). A and C show these two phenotypes in an orthoslice in the middle plane of the embryo, while B and D show a 3D reconstruction. B is seen from above (dorsal view) and D is seen laterally, with a plane cutting through the middle of the somite. Immunohistochemistry for N-cadherin on A&B and for Phalloidin on C&D.

These phenomena happened both in *cbr-* and $\Delta 390$ treated embryos though with different frequencies (Fig.10). Occasionally fissions were seen also in control embryos, in the anterior-most somites of control embryos, though with a much lower frequency (Fig.10A). While fissions were slightly more frequent in *cbr-* treated embryos (40% of the embryos analyzed had fissions against 37% of $\Delta 390$ treated embryos; Fig.10A), fusions are more frequent in $\Delta 390$ (with almost 50% of the embryos affected versus 40% in *cbr-*). Fusions were never observed in control embryos. The fissions tend to happen in the most anterior somites for all conditions, but were also found in S8, S11 and S12 (Fig.10B), while fusions happen more between somites S5-12 (Fig.10C).

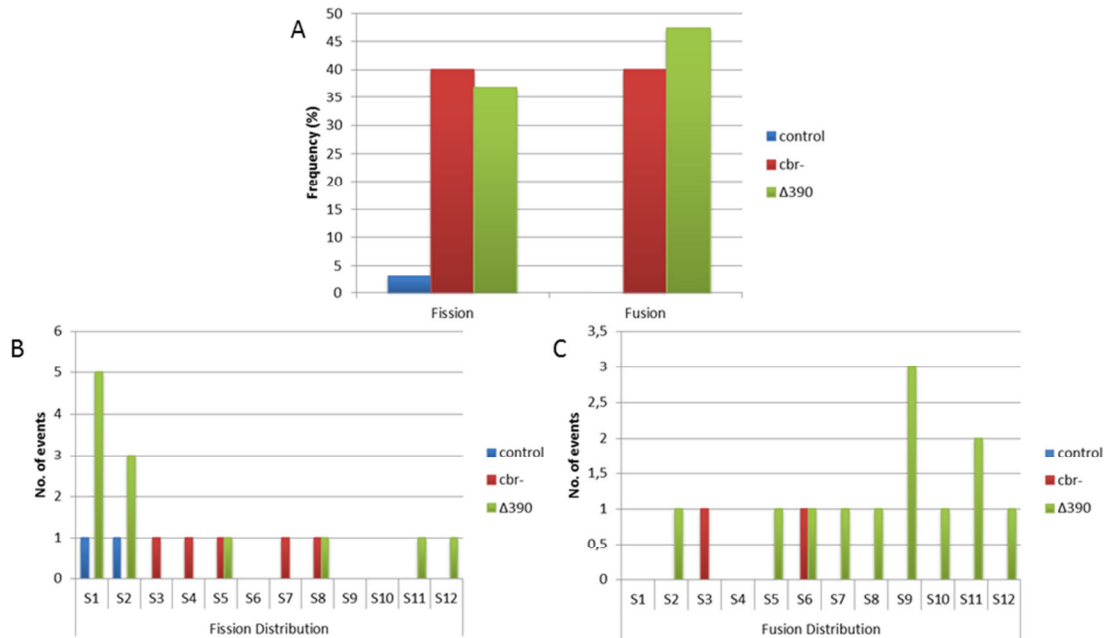


Fig.10 Graphs of the frequency of embryos affected with fissions and fusions in both treatment and control embryos (A) and the distribution of these two phenomena along the antero-posterior axis (B and C)

Other phenotype observed was the presence of labeled cells in the vicinity of the somite, but not inserted within the epithelial wall. This phenotype was observed exclusively in embryos electroporated with $\Delta 390$ and only in seven embryos out of 34 analyzed. Presumably these cells had abandoned somite and were unable to re-attach, which could

provide a possible explanation for smaller sizes of some somites measured. The most severe case is shown in Fig.11, an embryo electroporated with $\Delta 390$ and immunostained for N-cadherin. These “stray” cells were counted in four somites in each embryo, four embryos out of seven and the counts are shown in Table III. In the most severe case (Fig.11A&B), the average number was around the 45 cells per somite; taking into account that each somite has around 2000 cells (Venters et al., 2008), this represents a mere 2.2% difference in volume, clearly not accounting for the differences in size of the somites detected. Also, this phenomenon was not restricted to the last formed somites which is where I measured the smallest somites.

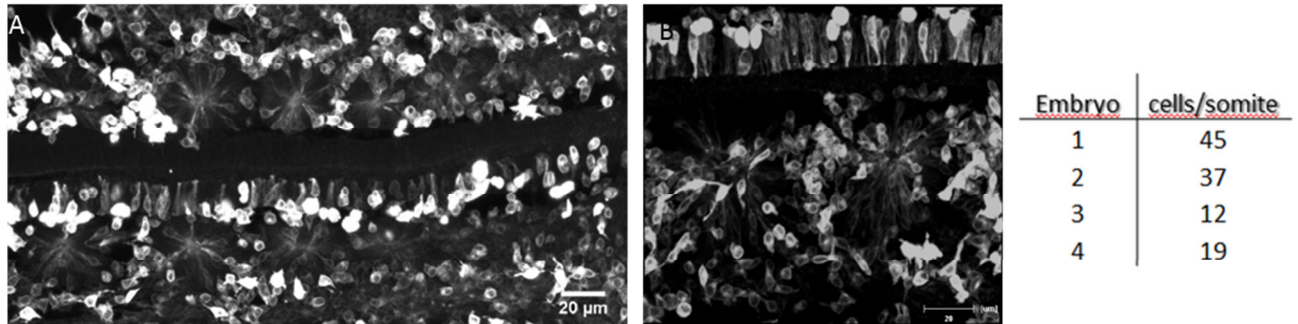


Fig.11 Caudal portion of a $\Delta 390$ electroporated embryo showing a large number of cells outside and around the somites (A). A detail of a medial portion of the embryo is shown in B, with the somitic cells marked with $\Delta 390$ and positive cells all around. Table shows the average number of cells around each somite for 4 embryos analyzed.

To better understand if the effects of the dominant negatives were due to effects on cell compaction and/or organization of the epithelial/somitocoel compartments of somites, a mesenchyme-to-epithelium ratio was calculated and compared for the previously selected somites between treatments. To do this, the volumes of the somitocoel vs. the epithelial portion of the somites were obtained from the 3D reconstructions (Fig.12A-D). In the other two combinations of somites, the results did not show big differences between treatments and control, so I focused all the following analysis in the combination the somite combination S16-S18. In the case of the last formed somites, the ratio was smaller in treated embryos (Fig.12E; S16-S18), with stronger effects in the $\Delta 390$. This could result either from an impaired distribution of cells between the somitocoel and epithelium (with more cells in the epithelia rather than in the somitocoel) and/or to effects of compaction of cells in these two compartments (less compaction leading to larger epithelia, ergo smaller ratios). Seeing the values separately, a decrease in the somitocoel volume occurred in the $\Delta 390$ treated embryos, but not in the *cbr-* treated embryos. In this case, the smaller ratio is explained by the considerable increase of the epithelium volume (more than the double of the volume seen in the control embryos) (SV of Sup.Mat).

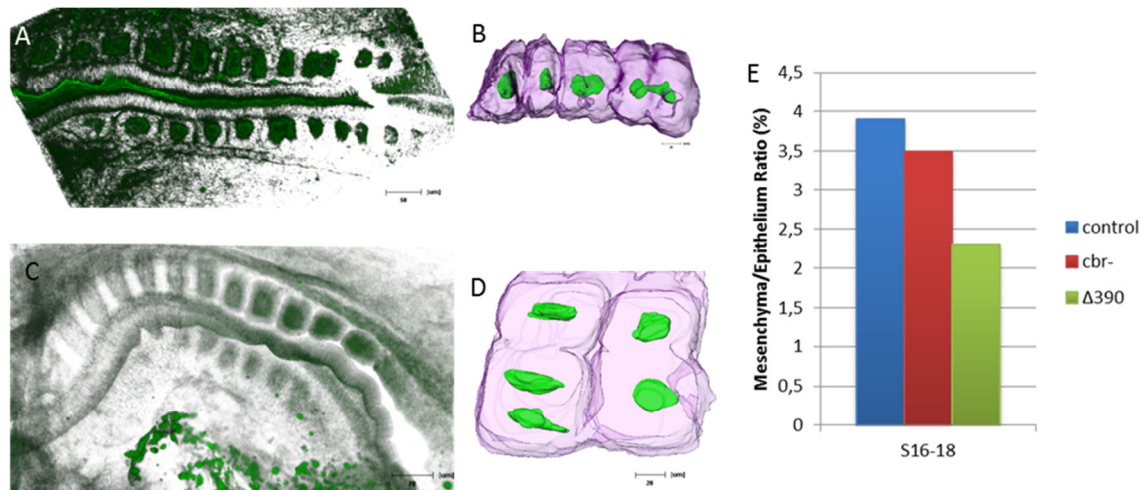


Fig.12 Volume reconstruction and calculations of mesenchyme/epithelium volume ratio of a $\Delta 390$ treated embryo (A) with a detail of the somites S11-16 (B) and a *cbr-* treated embryo (C) with a detail of somites S3-4 (D). In B) and D), somitocoels are shown in green and epithelium surface in purple (transparent). E) shows a graph where the volumes of somitocoel and epithelium were compared for the treated and control embryos for the combination of somites S16-18. Average values on SV of Supp.Mat.

To correlate the above results with the differences observed in somite sizes, a preliminary analysis of the morphology and compaction of the epithelia was done. The results are shown in Fig.13 and suggest that the somitocoel has less cells in both treated embryos than in control embryos (Fig.13D), which could explain the smaller size of the somitocoel and the decrease in the ratio as observed above for the $\Delta 390$. The epithelia of *cbr-* treated embryos seemed to be more disorganized (Fig.13B), with more cells in the same portion of epithelial wall and the nuclei were more rounded than those found in controls. This seems to explain the larger size of these somites.

Though the somites of $\Delta 390$ treated embryos are shorter (and not wider) than controls, analysis of cell compaction actually suggests that they contain more cells per same section of epithelium, which at first seems contradictory, but the nuclei are highly elongated and with a high degree of compaction. Also, the rostral and caudal epithelia seem to be thinner, with all the nuclei at the same apical-basal level and losing the pseudo-stratified structure typical of controls (Fig.13C&D). In fact, though these somites are significantly less long than controls, their total volume is not significantly smaller, since what they lack in length is compensated by thickness dorso-ventrally (Fig.7). The average volume of control somites was $131\,649,9\mu\text{m}^3$, while a $\Delta 390$ -treated had an average of $137\,314,6\mu\text{m}^3$ (SV of Supp.Mat), and potentially more cells overall. Clearly the lack of extracellular domain of some cells results in a different organization of the epithelium, which accompanies the final shape of the somite – more compacted rostro-caudally.

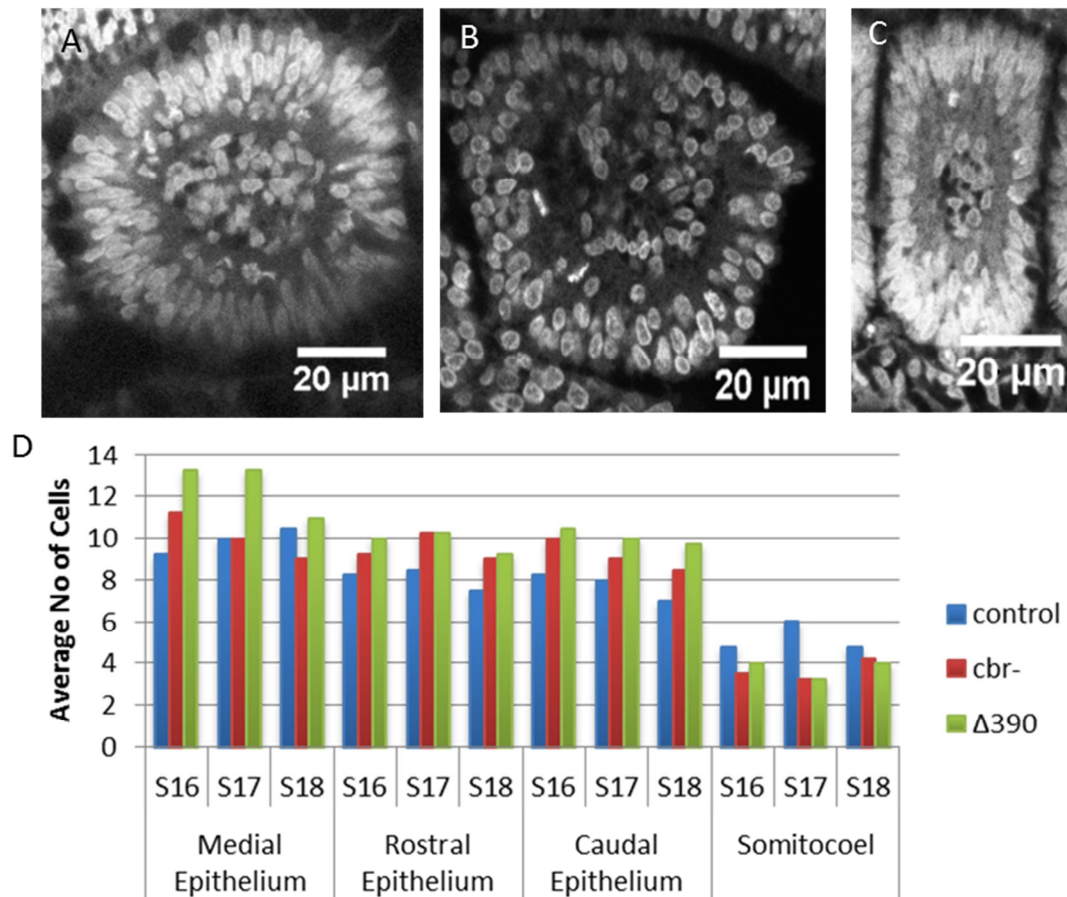


Fig.13 Average number of cells in the medial, rostral and caudal epithelium and in the somitocoel. Cells' nuclei were counted along a line of 25um across each epithelial wall, and 20um in the somitocoels in the "equatorial" plane for each treatment - control (A), cbr- (B), Δ390 (C) – in the three more posterior somites (S16-18). Average values on SVI of Supp.Mat.

III.2.4 Effects on Somite Formation

By co-electroporating embryos with dominant-negative constructs and GFP we were able to film embryos live and track cells with N-cadherin affected. One live-imaging of an embryo electroporated with Δ390 showed two interesting phenomena: first, a Δ390-positive cell that was in a formed epithelium lost the ability to attach and abandoned the formed somite, and second, a collision between a forming somite (S0) and a formed somite (SI) induced the loss of the rostral epithelium in the SI when collided with SII (Fig.14). What happened to the cell (red circle in Fig.14A) could be the explanation of the phenotype described previous in Fig.10, and there are other cells visible around the somites that could have had the same fate. As for the collision, S0 (yellow) suddenly starts moving in direction of SI (green), pushing it against SII (blue) and making the whole rostral epithelium to collapse (see also SVII in Supp.Mat.). Though the rostral epithelium still forms, it is typically thinner than it should be (Fig.13C compared with A), which might indicate that it needs the extracellular domain of the N-cadherin to be stable and normal. The lack of the extracellular domain could be the factor that explains why the epithelium collapsed in this case. This observation suggested that somite clefts

are first formed without noticeable effects and epithelialisation of the somatic wall progresses, but then collapses leading to fusions and fissions as seen in the more mature somites.

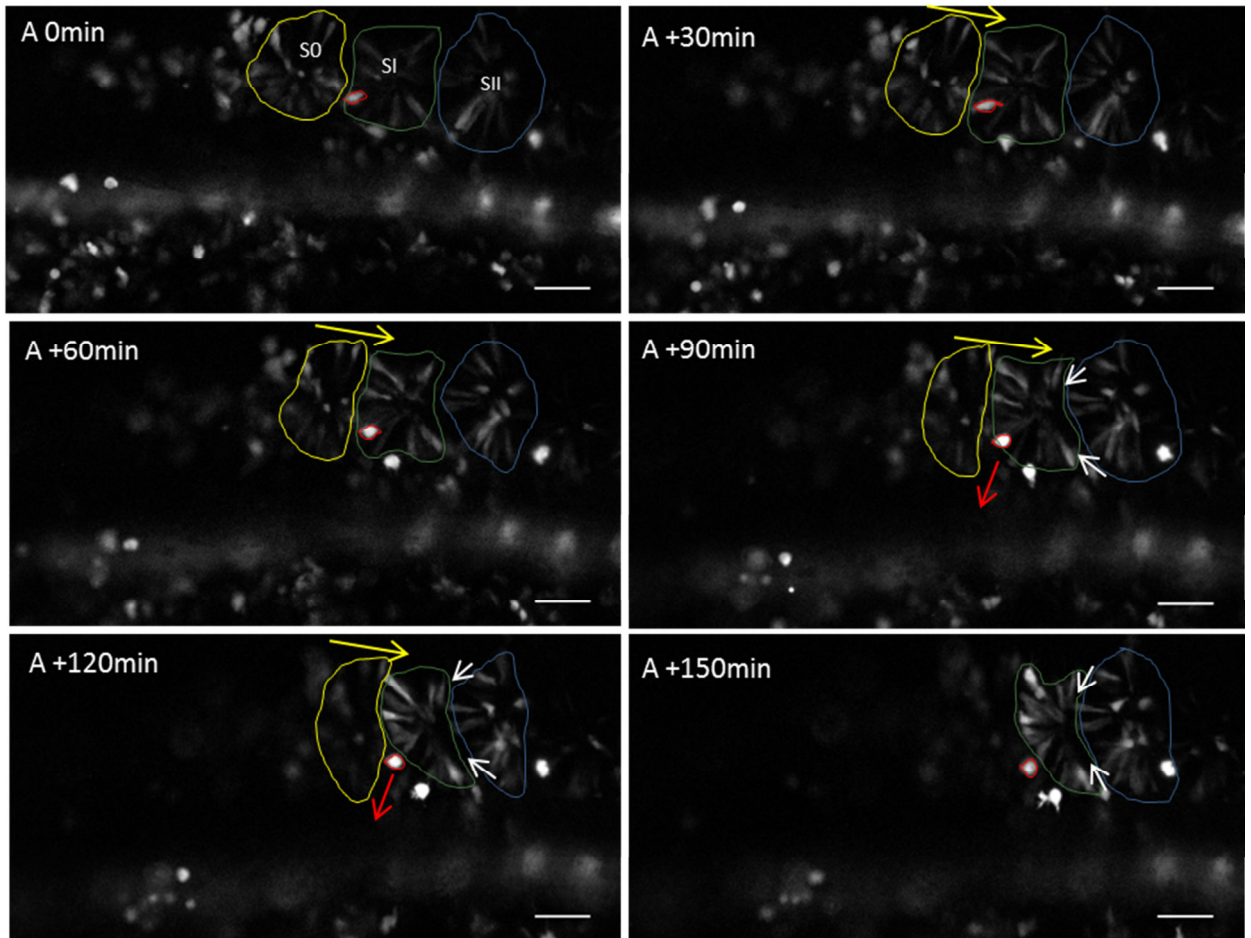


Fig.14 Collision between S0 (yellow), SI (green) and SII (blue) and "jumping" cell (red) in a $\Delta 390$ treated embryo. For more details see also SVII in Supp-Mat. A) Panels represent six time-points (spaced 30 minutes) of a 4D confocal imaging sequence of embryos expressing a mosaic of $\Delta 390$ +GFP-positive and negative cells. Posterior is to the right and anterior is to the left. Yellow arrow shows the movement done by S0 while colliding with the SI. Red arrow shows the movement of the "stray" cell as it abandons the epithelium. White arrows point to the local where the fusion is happening.

III.3 Expression Pattern of Cad11 and N-cadherin

The expression pattern for both molecules was observed in chick embryos of stages HH8 to HH12, to compare embryos with 10 or less somites and embryos with more than 10 somites. I used two different protocols for developing the *in situ* hybridization protocol: the BM-Purple and the Fast-Red. The BM-Purple embryos were either observed *in toto* or processed in a cryostat and observed in transversal or sagittal sections, while the FastRed-processed embryos were observed with the confocal microscope, which allowed for 3D reconstructions of the pattern of expression, as well as quantifications of fluorescence. Both methods for developing the embryos originated images that showed patterns of mRNA detection that were consistent.

III.3.1 Cad11 mRNA expression pattern

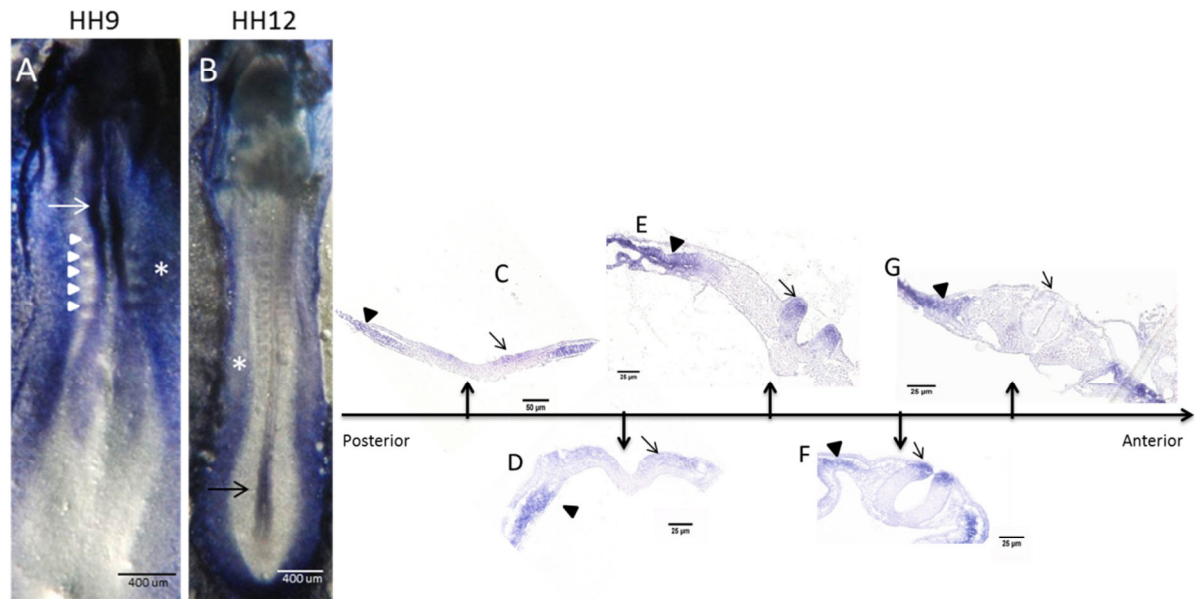


Fig. 15 General expression pattern of Cadherin11. The expression pattern was shown in whole mount of stage HH9 and HH12 (A and B) and in transverse sections from a more posterior position (C) to a more anterior position (F). It expresses mainly in the lateral mesoderm (A and B, asterisk; C-G, arrowheads) and in the neural plate (C, arrow), neural folds (arrow in D) and posterior portion of the neural tube (E and F, arrows), disappearing when the neural tube is fully closed (G, black arrow). The expression in the neural tube moves from a more anterior position (A, arrow) to a more posterior position (B, black arrow). Transiently expression in the somites is detected in HH9 embryos (A, arrowheads). C to G were assembled to demonstrate the expression pattern in the sequence of events that originate the neural tube; they do not belong all to the same embryo or to the same developmental stage but represent the typical pattern seen.

III.3.1.1 Other tissues

Cadherin11 expresses mainly in the lateral mesoderm and in well-defined bands in the neural tube (Fig.15, arrows). For the studied stages, I never found expression in the endoderm or ectoderm. The expression on the lateral mesoderm seems to be quite stable throughout the stages observed (Fig.15A&B*; C-G arrowhead), while the expression on the neural tube shifts posteriorly along the antero-posterior axis (Fig.15A&B, white and black arrows) and dorsally along the dorso-ventral axis (Fig.15D-F, black arrow). This pattern could be associated with the formation and closure of the neural tube processes (Van Straaten et al., 1996). The expression starts in the neural plate in the posterior part of the embryo. While shifting anteriorly, the neural fold starts forming and originates the neural groove, both being positive for cad11 (Fig.15D, black arrow). The neural folds became thickened and start to approximate, and as this occurs the expression of cad11 switches from the ventral to the most dorsal part of the neural tube, eventually concentrating at the tips of the neural fold. This expression is maintained at the sites where the neural tube is adhering and fusing. Then, after the fusion of the neural tube, it remains only residually expressed in the apical part of this structure, until it eventually disappears (Fig.15G, black arrow).

III.3.1.2 Paraxial Mesoderm

Cad11 mRNA was never detected on the presomitic mesoderm at any of the stages observed (HH7-HH13), and it was only faintly detected on somites of embryos at HH9 (Fig.15A&16A, arrowheads; Fig.16B&C, arrowhead in transverse section and 3D reconstruction). This expression occurs in the lateral side of the somites (Fig.15B&C). Though faint, it expresses more strongly in the anterior somites than in the posterior ones. In older embryos, the expression disappears completely from the paraxial mesoderm (Fig.16D&E). Also, contrarily to what we saw with N-cad (see below), cad11 does not appear to be involved in gastrulation, since there is no expression in the node (Fig.16A&E).

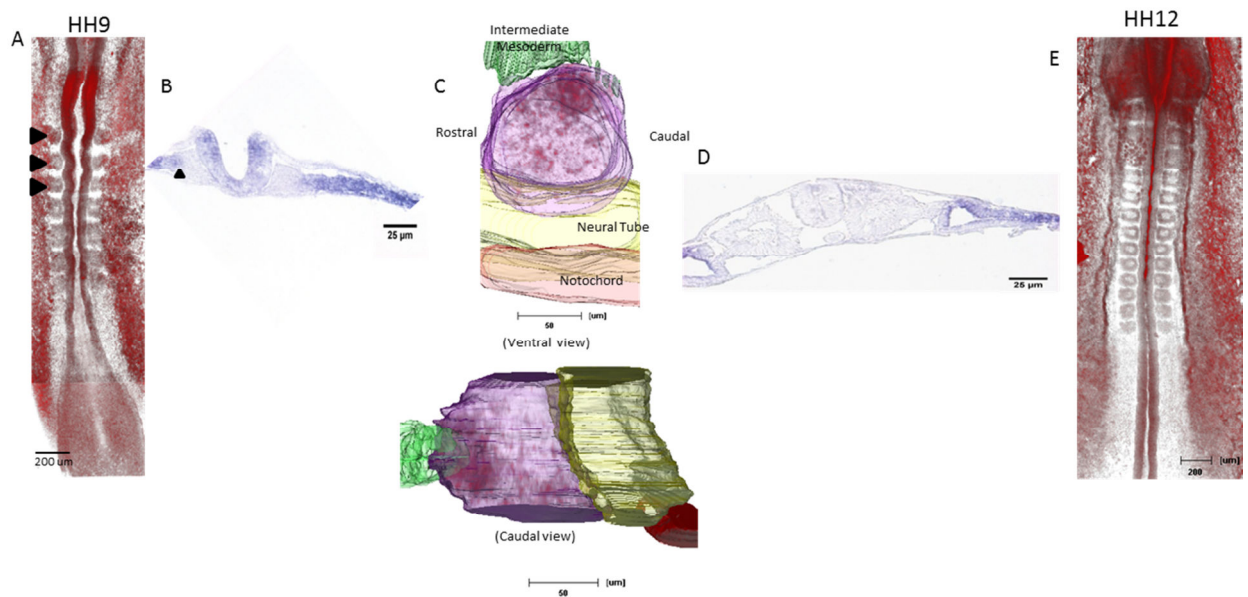


Fig.16 Cadherin 11 expression pattern in the paraxial mesoderm. It is never expressed in the PSM (A and E) and it only expresses transiently in somites (A, Fastred development, and B, transverse section, arrowheads). This expression is positioned more lateral in the somite (C, ventral and caudal view, red inside the somite in purple). After this stage, it disappears from the somites (E, whole mount developed with Fastred; D, transverse section).

In conclusion, based on the observation of patterns of mRNA expression in the PSM of chick embryo from stages HH7-HH13, cad11 is not involved in paraxial mesoderm formation or maturation into epithelial somites, though it may play a role in the intermediate and lateral mesoderm, and in the neural tube closure. Given that I detected expression in somitic cells, it is possible that cad11 plays a role in maintaining cell cohesiveness and in separating lateral somitic cells from intermediate mesodermal cells. To our knowledge, this expression has so far not been reported in the literature. Clearly, if other cadherins cooperate with N-cadherin during chick somite epithelisation, Cad11 is not one of them.

III.3.2 N-cadherin mRNA Expression Pattern

The N-cadherin molecule expresses in many tissues during the early embryonic stages up to HH13, such as the head, neural tube, notochord, intermediate mesoderm, node and paraxial mesoderm. The expression pattern in these tissues has already been documented (<http://geisha.arizona.edu/geisha/>), so I will focus my observations on the expression in the paraxial mesoderm. Here, the pattern changes as the somite matures.

III.3.2.1 Before and After 10 Somites

In both cases, the expression on the presomitic mesoderm is stronger in the caudal part than in the middle portion, increasing again in the rostral-most PSM where a new somite is forming (S0; Fig. 17A,C&G). In embryos with less than 10 somites (<HH10), the last somites formed show a strong expression of the N-cadherin mRNA (Fig.17A&H, top embryo), with higher levels than those found along the PSM. The expression establishes preferentially in the anterior part of newly formed somites, while the expression in the posterior remains lower (Fig.17C&D, white arrows). These characteristics seem to be constant since the last five somites formed in each stage are the ones that retain expression specifically in the anterior part (Fig.17C,D,E&G, arrows). As somites mature, the expression homogenizes through the epithelium, while the somitocoel always retains low expression levels (Fig.17G, asterisks). When the ventral portion of the somite dissociates to form the sclerotome, the expression is downregulated and is only maintained in the dermomyotome. Although it has been reported that medial PSM cells show precocious signs of epithelialization (Martins et al., 2009) we did not find evidence of increased levels of expression of N-cadherin- in these cells when compared to lateralmost cells of the PSM, which suggests that this epithelialization is not N-cadherin dependent.

As for the observation of the protein (through IHC), it appears to accumulate in cells close to the node immediately after their ingression to form mesoderm (Fig.17H, green embryos). High levels of N-cadherin protein are maintained throughout the posterior-most PSM, but begin to decrease in the middle part and increase again in the rostral-most PSM, where new somites are becoming epithelial, accompanying the pattern of mRNA expression. However, N-cadherin protein accumulates first in the caudal part of the somite, where the epithelium is already formed (Fig. 17I). When the somite is fully epithelial, the protein accumulates in the anterior epithelial also, possibly caused by the peak of mRNA expression seen in these cells during somite epithelialisation (Fig.17D). When the sclerotome starts to dissociate from the dermomyotome, expression is only maintained in the dermomyotome (Fig.17F). Despite the fact that the mRNA seems to decrease in the most mature somites, such tendency is not seen in protein levels, as detected by immuno-fluorescence.

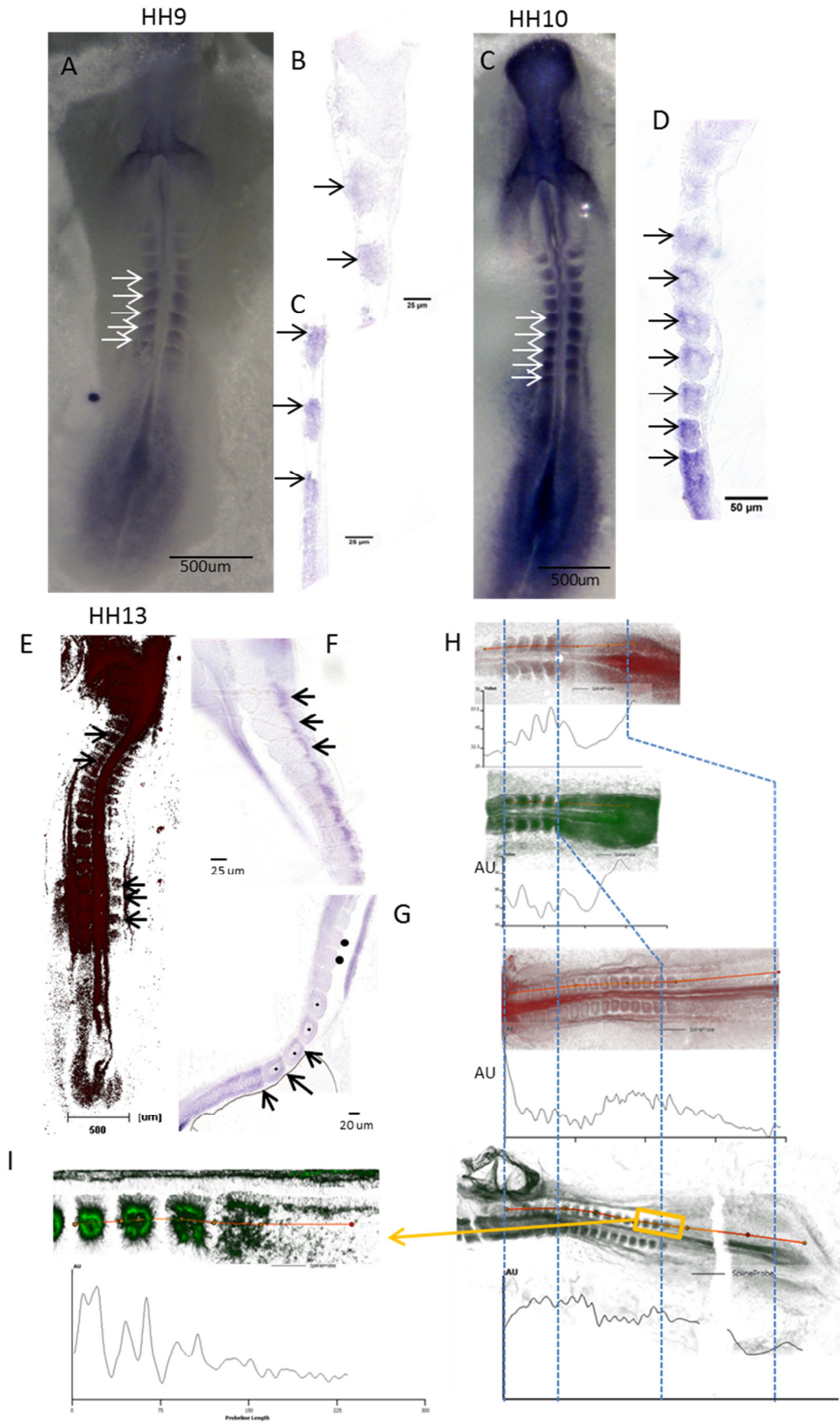


Fig. 17 IHS for N-cadherin and comparison between mRNA and protein expression profile. For younger embryos (HH8 to HH10), N-cadherin mRNA expresses in the node and in the more posterior portion of the PSM,

decreases in medial PSM and regains expression in the rostral part, where the new somite is being formed (A and C). It accumulates preferentially in the anterior part of the forming somite and also in the more recently formed somite (A, C and E, white arrows; B, C, D and G, black arrows) and homogenizes later in development, while the somitocoel always retain low levels of expression (G, black dots and asterisks, respectively). In older embryos (HH12 and 13), as the somite matures, the expression homogenizes and increases only in the dermomyotome (F, black arrows), while downregulates in the sclerotome. Also, the tendency on the PSM is reversed, with increasing expression throughout the medial portion. H shows the expression profiles for the mRNA (red) and the molecule (green) in an HH8 and an HH12 embryos. Like the expression of mRNA, for younger embryos the protein also expresses more in the caudal PSM, decreasing in the medial portion and increasing in the rostral portion. Unlike the mRNA expression, the protein expresses more in the caudal part of the forming somite and of the most recently formed somites. The homogeneous expression only happens when the somite is fully epithelial. I is a detail of the region marked with a yellow square.

IV - Discussion

IV.1 Comparing the Two Techniques: electroporation *in New* and *in ovo*

Since N-cadherin is expressed in cells when they gastrulate, there was a possibility that impairing N-cadherin would affect gastrulation. Therefore, it was interesting to observe cells positive for the two dominant negative constructs incorporated within the PSM and somites which shows they are capable of gastrulating and move within the paraxial mesoderm. There are several possible explanations for this: i) Either N-cadherin is not necessary for gastrulation, ii) expression of the constructs builds up only gradually so electroporated cells have enough time to gastrulate before “critical” levels of the dominant negative form accumulate, or iii) endogenous expression of *wt* N-cadherin is sufficient to maintain “normal” cell functioning during gastrulation. The fact that treatment with *mncd2* or the knockout experiments does not appear to cause major effects during gastrulation suggests that N-cadherin is indeed not essential. Also, after electroporation expression levels typically peak around 12-24h, so there is a buildup that is necessary for the effects of dominant negatives to be seen. It turns out that, for our experiments, the maximum of effect occurred exactly while electroporated cells were being incorporated into new somites and maturing.

The truncated vectors used in this study have YFP (Yellow Fluorescent Protein) in frame instead of GFP, which is not optimal for imaging in our microscopes. Also, we noticed that despite the concentration of the vectors being similar to those of the control GFP vector, the expression levels were typically lower which made it difficult to perform live imaging. To address this we tried co-electroporation with the GFP vector. Although I could not find a specific paper about this issue, it seems to be common practice to electroporate the vector of interest with a normal pCAGGS-GFP.

IV.1.1 In New vs In Ovo

Clearly each method of culture has its own advantages and disadvantages, namely the access to correct staging of embryos and identification of anatomical features, the efficiency of electroporation and the number of embryos that can be collected with each experiment. I found electroporation *in ovo* easier and faster, and potentially less harmful for the embryo. However, the *New* technique has other advantages: First, the embryo is fully exposed, so the staging and correct identification of the desired area is easier and quicker. Also, when choosing for confocal live-imaging, the embryo is already outside the egg and is easier to manipulate, and image, allowing bright-field images. There is one difficulty though: because the embryo is exposed ventrally, I found it more difficult to deliver the vector to cells in the primitive streak.

One important difference between the two cultures, and which, despite its importance we did not account for, is that the embryos are subjected to different levels of tension *in*

ovo and in *New* which may affect size and shape of embryos (Stern and Bachvarova, 1997). In our case, most control embryos were processed in *New*, while *cbr-* was in *ovo* and $\Delta 390$ was a mixture of both. Though there is a possibility that there is a “culture” effect masking our results, since the phenotypes were consistent in $\Delta 390$ we considered this not to be an important effect. Future experiments should address this possibility by measuring embryos cultured *in ovo* and in *New*.

In this work I was faced with two other major difficulties: frequent contaminations, a serious problem in both techniques, and an apparently inexplicable developmental arrest in most cultures initially. The incubation time for bacterial infection is around the six hours, which incapacitates the normal flow of experiments. To avoid it, all the material and solutions should be sterilized and, in case of the *new*, the rings should be kept in ethanol (~60%). Normal effects of contaminations, in the case of the *new* technique, include permeabilization of the vitelline membrane, detachment of the blastoderm from the vitelline membrane and even, in the most serious cases, total degradation of the embryo. In the case of the culture *in ovo*, although less frequently, it also happened and the usual effect was the destruction of the embryo, extreme dryness and strange colours and texture. The second problem was solved by allowing embryos to “wait” at room temperature instead of trying to keep them at 38°C during the whole procedure (thanks to the expert advice of Raquel Mendes).

IV.2 Functional Impairment of N-cadherin

IV.2.1 Experimental Setup

The initial experimental design included observing multiple embryos of all possible stages, which proved to be too complex to analyze. Though I studied embryos that were initially at HH3-HH8 and culture times as long as 36h, comparing those introduced noise in the results since in some cases the somites that were being compared were at different maturation levels. Therefore, the embryos used in the final analysis were only those electroporated from stage HH4-HH6, and which were cultured for 24-28h. This ended up excluding several control embryos and many of the *cbr-* treated embryos that were electroporated *in ovo*. For the case of the *cbr-*, electroporation *in ovo* seemed to be the only technique that produced good results in the end, maybe because in the *New* technique this vector would dilute much faster than the others. Since I have not confirmed that the two techniques do not introduce differences between embryos (as explained above), I cannot rule out the possibility that differences seen between control and *cbr-* treated embryos are also due to culture effect. Embryos treated with *mncd2* were all excluded from the analysis since no major defects were found when analyzing the embryos. There is always a question of permeabilization to the antibody and that might be a good reason for this. Still, I would expect even a small percentage of embryos affected, has described by Linask et al. (1998), which led me to conclude that maybe the antibody that I used was not in the best condition.

After this pre-selection, the statistical analysis showed more reliable differences between treatments and controls. Though it is possible that comparing somites of the same axial position without using always the same exact initial stage and culture time could not be the best approach, it revealed differences that would not be detected otherwise if I had focused my observations on a single specific somite or stages. Especially if I had chosen to analyse S10-15, which are the ones better characterized in our lab, but which apparently are the ones which show the least defects by the treatments done in this work. Also, since in the literature there have been differences reported in the behavior of somites S1-10 and S10-20, it was important to analyze embryos that included those two different stages.

IV.2.2 Different vectors, different phenotypes

Interestingly, in the end, the two dominant negative vectors seem to affect somitogenesis in different ways and produce different kinds of defects. In the case of the $\Delta 390$, the construct without the N-cadherin extracellular domain, the number of somites formed was in some cases higher and in others lower than the number expected, and the last formed somites were consistently smaller in length, while for the *cbr-* (the construct without intra-cellular domain), embryos formed less somites than the expected and they were generally bigger. Though the formation of more somites than the expected could be an artifact of culture or errors in staging, the fact is that this only happened for the $\Delta 390$. If it was an error, it would happen with the similar frequency in the other treatments. Also, the occurrence of fusions or fissions was usually not correlated with embryos making more or less somites for neither of the vectors. This raises interesting questions: why the lack of the extracellular domain leads to posterior somites that are smaller in length and bigger in height while the lack of the intracellular domain (*cbr-*) originates bigger somites throughout the embryo?

It would be reasonable to expect that cells without the extracellular domain of the N-cadherin were not able to establish strong adhesions between them, while cells that have an overexpression of the extracellular domain ($\Delta 390$ electroporated embryos) would have an “excess” of adhesions. However, my data suggests that what happens is exactly the opposite, since the medial epithelial wall of somites in which cells lack the extracellular N-cadherin domain is more tightly assembled while the other epithelia are more loose and disorganized. One possible explanation for this case would be the fact that maybe other adhesion molecules compensate for the lack of N-cadherin function. Also, the fact that the intracellular domain is overexpressed could be affecting the actin cytoskeleton, inducing the accumulation of adhesion belts and increasing the cortical tension of the cells, or even preventing them from moving as they normally would (see Martins et al 2009). To address this question it would be informative to study the actin cytoskeleton of these cells and see if there is a peak of accumulation or a different distribution of F-actin; my images with phalloidin staining were not conclusive in this respect.

The rostral and caudal epithelia seem thinner and the nuclei are more aligned and less pseudo-stratified as in control somites. This could happen because cells without the extracellular domain are not able to position themselves correctly. In fact, these somites of $\Delta 390$ treated embryos are bigger in the dorsal-ventral thickness than controls and this could happen because cells are being misplaced. Since accretion plays a major role in the assembly of this epithelium and it clearly involves cell-cell interactions, maybe this process is not being done efficiently, recruiting fewer cells or misplacing them. This would make sense if cells in fact needed the extracellular domain to correctly orient and position themselves. It would be interesting to study more profoundly the morphogenetic movements of these cells as they give rise to the somite; eg., track cells and compare their dynamics of those of control cells.

Also interesting was the observation that $\Delta 390$ affected somites along the antero-posterior axis in different ways, as the somites between S11-S14 are bigger than those of S16-S18, which could mean that in this epithelium cells lose compaction because of the extracellular domain is not present to maintain the cohesion. Though I did not count the total number of cells in the epithelia or studied closely their morphology in these somites, this would be interesting to do and assess if the cell morphology is in fact different. If this is the case, then it would suggest that when the somite forms the connection with the cytoskeleton is important for the correct morphogenetic movements to happen and this would be guided by temporary connections mediated by the extracellular domain, while later on, the extracellular domain would be necessary mostly to maintain the normal cell compaction of epithelia. As a matter of fact, for the formation of the sclerotome to happen, compaction has to decrease on the ventral side of the somite. And for that, N-cadherin has to be downregulated on the ventral side – without it, sclerotome would not probably form in the right position and time.

In the case of the *cbr-* treated embryos, somites are bigger throughout the embryo. One way to explain this could be the fact that cells are more loosely distributed in the somite epithelium, possibly because the lack of the intracellular domain induces a more “relaxed” cell morphology. By observing the nuclei shape, this seems to be the case – nuclei seem more round-shaped in *cbr-* treated embryos than in the control. To better understand this, it would also be important to look better for the epithelium, marked for the N-cadherin and the F-actin, calculate the length/width ratio of the cells and try to capture the formation of *cbr-* treated somites through live-imaging. Either way, in both cases, the intracellular domain seems to play an essential role for the correct morphology of the somite. Further analysis is necessary to determine how.

IV.2.3 Fissions and Fusions

Both phenotypes are seen in the two treatments, which suggest that both domains of N-cadherin are important for maintaining somite cohesiveness. In both cases, the effects in the rostral and caudal epithelia seem to be the cause for these phenotypes. When two somites fuse and share a common somitocoel, this implies the collapse of one caudal and one rostral epithelium, and the establishment of adhesions between epithelial cells

that otherwise would not touch each-other, because they are at different sides of the inter-somitic border. This seems to be confirmed by the time-lapse observations, where a somite SI forms normally but then the rostral epithelium collides with the caudal epithelium of the somite SII and collapses. Still, it is often visible that the rostral somite is more prone to collapse. This hypothesis will be further discussed later. The better way to be sure of this would be to analyze more time-lapse movies of the effect and further investigate the cell movements by cell tracking.

In the case of the fissions, since they seem to happen only in rostro-caudal axis (ie, a somite always splits sideways), I argue that this is also a sign of collapsing of rostral and caudal epithelia, followed by an abnormal epithelialization in between the two halves (for example by condensation of somitocoel cells into epithelia). Unfortunately I never found an example of the phenomenon in the middle of its progression in fixed embryos, or find it happening in the time-lapse movies. It is also possible that instead of this representing a fission of an already formed somite, that two somites form at the same time on one side from an already split PSM, though I never found evidences of fissures in PSMs. Also according to (Freitas et al., 2001), only the medial side of the PSM has the capacity to originate somites. So this hypothesis does not seem plausible.

Either way, this somite phenotype seems to corroborate the idea that impairment of the N-cadherin affects preferentially the rostral and caudal epithelial walls and affects cell positioning and strength of the structure. Since in these epithelial is where cell accretion happens the most, this could be indicative that this movement is indeed affected, by wrongly deposition of cells in this epithelium. Fissions along other axii were never found (ie, rostro-caudal or dorso-ventral splits), which again argues that the dorsal, ventral, medial and lateral walls are less prone to defects caused by N-cadherin impairment.

IV.3 Expression Pattern of Cad11 and N-cadherin

IV.3.1 Cad11 mRNA Expression Pattern

Cad11 seems to have distinct different roles in the chick embryo when comparing the expression patterns with those of mouse embryos. In the mouse, cad11 appears in somites and contributes to their correct epithelialization (as suggested by knockout experiments), though clearly less than N-cadherin (Horikawa et al 1999). As the somite develops and matures, the expression of these two molecules became complementary: N-cadherin remains in the dermomyotome while cad11 is expressed in the sclerotome. Cad11 seems to be associated with the osteoblast lineage, playing a role in the mineralization and cell differentiation (Kimura et al., 1995; Horikawa et al., 1999; Kii et al., 2004). In chick embryo, the expression of the Cad11 molecule in somites is much more restricted in place and time, only happening in the lateral part of the somite for a short period of time (the only expression detected occurred when the embryos had between 6-9 somites). No expression was ever detected on the sclerotome, though we

did not study advanced stages of sclerotome formation. The initial hypothesis of the project was that cad11 would be expressed in the paraxial mesoderm of embryos with more than ten somites and cooperate with N-cadherin during the epithelialisation, which would explain why somite 10 and beyond seemed to be more resistant than the first ten to N-cadherin impairment (Linask et al 1998). My results clearly showed that this is not the case. Unfortunately there are no known antibodies against the chick version of the protein to confirm these observations, or a method to impair its function in chick. My observations suggest that cad11 may play a role in the definition of the boundary between the intermediate mesoderm and the lateral-most somatic cells, helping on the separation of the two tissues. My observations also suggest that cad11 is important in neurulation, since its expression pattern seems to correlate well with the timeframe of this process. According to the work of Van Straaten et al. (1998), the process of closure has a multiphasic pattern, with independent closure events that occur throughout the axis of the embryo, contradicting the zipper-like model. This process implies the longitudinal extension, the transversal constriction and the apico-basal thickening of the neural plate. After that, the lateral borders of the neural plate elevate and the neural folds converge to the midline. For this to happen, cells suffer an apical constriction and medial and dorsolateral hinge points have to form. In the end, neural folds come together in a process called apposition, adhere and then fuse in the midline. Each of these three moments takes their own time to occur. Cad11 is not only present in the neural plate, but also accompanies the arising of the neural folds, concentrating its expression pattern on the very tips of the folds while they are adhering, maintaining its expression even after the fusion of the neural folds. Eventually it fades out, after the neural tube is already fused.

IV.3.2 N-cadherin mRNA Expression Pattern

I attempted to estimate levels of N-cadherin expression and protein accumulation by measuring profiles of fluorescence in Fast-red ISH processed, and IHC processed embryos, respectively. This was attempted to try to better understand how the different defects seen in somites at different axial levels could be correlated with the axial profile of N-Cad expression. Both procedures rely on different principles: while the IHC uses antibodies that specifically bind to all the antigens present in a stoichiometric manner (and therefore more directly quantifiable), in developing of an ISH with a chromogen such as Fast-red the relationship between mRNA and signal detected is not linear, therefore quantification of fluorescence as a direct measure of mRNA levels is less reliable (Larsson, 1997). Despite the non-linearity nature of the process of mRNA detection, there is a reliable degree of confidence that in the same tissue, differences in detection levels correspond to differences of mRNA levels, in other words, an increase in the quantity of chromogen along the PSM correlates (though not necessarily linearly) with an increase in mRNA levels. A potentially more reliable technique for quantifying mRNA levels along the PSM and in somites would be to isolate these tissues and perform RT-PCRs.

The images and the analysis of mRNA profiles strongly suggests that N-cadherin is preferentially expressed in the rostral part of recently formed somites, while the protein accumulates first in the caudal epithelium of the forming somite and in the next somite formed. Only when the rostral epithelium is fully formed are the levels of protein expression homogenized in all the epithelium. An explanation for this could be that the rostral epithelium is more dependent on N-cadherin to epithelize and, since it forms later, there is a “boost” of N-cadherin expression during epithelialization of the rostral epithelial wall. One reason why this epithelium is more dependent of N-cadherin to maintain its integrity is that the intersomitic cleft forms without prior deposition of extra-cellular matrix (Martins et al., 2009), which would help cells settle and acquire a more epithelial behavior. All other walls of the somite are covered with extracellular matrix from early on in development, especially the medial, dorsal and ventral walls.

IN SUMMARY...

Impairment of different parts of the N-cadherin molecule can cause different somite “phenotypes”. The defects are less evident in the first thoracic somites. N-cadherin is not necessary for epithelialisation of the somite or formation of the intersomitic clefts, though it is important for maintaining somite epithelium integrity. Without it somites can collapse and split, or fuse with neighbors. The rostral and caudal epithelial walls seem to be particularly sensitive to N-cadherin impairment. The upregulation of N-cadherin expression in the rostral portion of the forming somite seems to corroborate this.

Curiously, without the extracellular domain some embryos form more somites than expected, though I did not find evidence of this being due to somite fissions.

Though the *mncd2* antibodies causes defects in early somites, the dominant negatives we tested caused effects on other somites also. Therefore, these vectors, assuming one can optimize their expression, have a better potential for revealing the role of N-cadherin in somitogenesis.

It would be interesting to study the effect of silencing translation of N-cadherin (morpholinos), since my observations suggest that overexpression of these truncated constructs can cause normal physiological side-effects such as increased adhesiveness (more extracellular domain) and contractility (more intracellular domain) in electroporated cells.

Cad11 is never expressed (contrarily to what has been described in mouse), and therefore cannot compensate for the lack of N-cadherin. Other cell adhesion molecules must cooperate with N-cadherin.

The role of N-cadherin seems to be more mysterious and interesting than previous results had suggested, influencing both cell morphology and adhesion and indirectly somite shape and somitogenesis.

V - References

- Aberle H, Schwartz H, Kemler R. 1996. Cadherin-catenin complex: Protein interactions and their implications for cadherin function. *J Cell Biochem* 61:514-523.
- Adams CL, Nelson WJ. 1998. Cytomechanics of cadherin-mediated cell-cell adhesion. *Curr Opin Cell Bio* 10:572-577.
- Bajanca F, Luz M, Duxson MJ, Thorsteinsdottir S. 2004. Integrins in the mouse myotome: developmental changes and differences between the epaxial and hypaxial lineage. *Dev Dyn* 231:402-415.
- Chuai M, Weijer CJ. 2009. Regulation of cell migration during chick gastrulation. *Curr Opin Genet Dev* 19:343-349.
- Cinnamon Y, Ben-Yair R, Kalcheim C. 2006. Differential effects of N-cadherin-mediated adhesion on the development of myotomal waves. *Dev* 133:1101-1112.
- Derycke LD, Bracke ME. 2004. N-cadherin in the spotlight of cell-cell adhesion, differentiation, embryogenesis, invasion and signalling. *Int J Dev Biol* 48:463-476.
- Duband JL, Dufour S, Hatta K, Takeichi M, Edelman GM, Thiery JP. 1987. Adhesion molecules during somitogenesis in the avian embryo. *J Cell Biol* 104:1361-1374.
- Freitas C, Rodrigues S, Charrier JB, Teillet MA, Palmeirim I. 2001. Evidence for medial/lateral specification and positional information within the presomitic mesoderm. *Dev* 128:5139-5147.
- Ganzler-Odenthal SI, Redies C. 1998. Blocking N-cadherin function disrupts the epithelial structure of differentiating neural tissue in the embryonic chicken brain. *J Neurosci* 18:5415-5425.
- Gates J, Peifer M. 2005. Can 1000 reviews be wrong? Actin, alpha-Catenin, and adherens junctions. *Cell* 123:769-772.
- Giacomello E, Vallin J, Morali O, Coulter IS, Boulekbache H, Thiery JP, Broders F. 2002. Type I cadherins are required for differentiation and coordinated rotation in *Xenopus laevis* somitogenesis. *Int J Dev Biol* 46:785-792.
- Grunwald GB, Pratt RS, Lilien J. 1982. Enzymic dissection of embryonic cell adhesive mechanisms. III. Immunological identification of a component of the calcium-dependent adhesive system of embryonic chick neural retina cells. *J Cell Sci* 55:69-83.
- Hamburger V, Hamilton HL. 1992. A series of normal stages in the development of the chick embryo. 1951. *Dev Dyn* 195:231-272.
- Hazan RB, Phillips GR, Qiao RF, Norton L, Aaronson SA. 2000. Exogenous expression of N-cadherin in breast cancer cells induces cell migration, invasion, and metastasis. *J Cell Biol* 148:779-790.
- Hirano S, Nose A, Hatta K, Kawakami A, Takeichi M. 1987. Calcium-dependent cell-cell adhesion molecules (cadherins): subclass specificities and possible involvement of actin bundles. *J Cell Biol* 105:2501-2510.
- Horikawa K, Radice G, Takeichi M, Chisaka O. 1999. Adhesive subdivisions intrinsic to the epithelial somites. *Dev Biol* 215:182-189.
- Horikawa K, Takeichi M. 2001. Requirement of the juxtamembrane domain of the cadherin cytoplasmic tail for morphogenetic cell rearrangement during myotome development. *J Cell Biol* 155:1297-1306.
- Ivanov DB, Philippova MP, Tkachuk VA. 2001. Structure and functions of classical cadherins. *Biochemistry (Mosc)* 66:1174-1186.
- Jamora C, Fuchs E. 2002. Intercellular adhesion, signalling and the cytoskeleton. *Nat Cell Biol* 4:E101-108.
- Kiener HP, Brenner MB. 2005. Building the synovium: cadherin-11 mediates fibroblast-like synoviocyte cell-to-cell adhesion. *Arthritis Res Ther* 7:49-54.
- Kii I, Amizuka N, Shimomura J, Saga Y, Kudo A. 2004. Cell-cell interaction mediated by cadherin-11 directly regulates the differentiation of mesenchymal cells into the cells of the osteo-lineage and the chondro-lineage. *J Bone Miner Res* 19:1840-1849.

- Kimura Y, Matsunami H, Inoue T, Shimamura K, Uchida N, Ueno T, Miyazaki T, Takeichi M. 1995. Cadherin-11 expressed in association with mesenchymal morphogenesis in the head, somite, and limb bud of early mouse embryos. *Dev Biol* 169:347-358.
- Larsson LI. 1997. Quantitative in situ hybridization. *Endocrine Pathology* 8:3-9
- Linask KK, Ludwig C, Han MD, Liu X, Radice GL, Knudsen KA. 1998. N-cadherin/catenin-mediated morphoregulation of somite formation. *Dev Biol* 202:85-102.
- Luo J, Wang H, Lin J, Redies C. 2007. Cadherin expression in the developing chicken cochlea. *Dev Dyn* 236:2331-2337.
- Martins GG, Rifes P, Amandio R, Rodrigues G, Palmeirim I, Thorsteinsdottir S. 2009. Dynamic 3D cell rearrangements guided by a fibronectin matrix underlie somitogenesis. *PLoS One* 4:e7429.
- Mège RM, Gavard J, Lambert M. 2006. Regulation of cell-cell junctions by the cytoskeleton. *Curr Opin Cell Biol* 18:541-548.
- Miyoshi J, Takai Y. 2008. Structural and functional associations of apical junctions with cytoskeleton. *Biochim Biophys Acta* 1778:670-691.
- Momose T, Tonegawa A, Takeuchi J, Ogawa H, Umesono K, Yasuda K. 1999. Efficient targeting of gene expression in chick embryos by microelectroporation. *Dev Growth Differ* 41:335-344.
- New DAT. 1955. A New Technique for the Cultivation of the Chick Embryo in vitro. *Journal of Embryology and Experimental Morphology* 3:326-331.
- Palmeirim I, Rodrigues S, Dale JK, Maroto M. 2008. Development on time. *Adv Exp Med Biol* 641:62-71.
- Provost E, Rimm DL. 1999. Controversies at the cytoplasmic face of the cadherin-based adhesion complex. *Curr Opin Cell Biol* 11:567-572.
- Psychoyos D, Stern CD. 1996. Fates and migratory routes of primitive streak cells in the chick embryo. *Dev* 122:1523-1534.
- Radice GL, Rayburn H, Matsunami H, Knudsen KA, Takeichi M, Hynes RO. 1997. Developmental defects in mouse embryos lacking N-cadherin. *Dev Biol* 181:64-78.
- Reynolds AB, Carnahan RH. 2004. Regulation of cadherin stability and turnover by p120ctn: implications in disease and cancer. *Semin Cell Dev Biol* 15:657-663.
- Scaal M, Gros J, Lesbros C, Marcelle C. 2004. In ovo electroporation of avian somites. *Dev Dyn* 229:643-650.
- Stern CD, Bachvarova R. 1997. Early chick embryos in vitro. *Int J Dev Biol* 41:379-387.
- Stockdale FE, Nikovits W, Jr., Christ B. 2000. Molecular and cellular biology of avian somite development. *Dev Dyn* 219:304-321.
- Takeichi M. 1988. The cadherins: cell-cell adhesion molecules controlling animal morphogenesis. *Dev* 102:639-655.
- Van Straaten HW, Janssen HC, Peeters MC, Copp AJ, Hekking JW. 1996. Neural tube closure in the chick embryo is multiphasic. *Dev Dyn* 207:309-318
- Venters SJ, Hultner ML, Ordahl CP. 2008. Somite cell cycle analysis using somite-staging to measure intrinsic developmental time. *Dev Dyn* 237:377-392.
- Voiculescu O, Papanayotou C, Stern CD. 2008. Spatially and temporally controlled electroporation of early chick embryos. *Nat Protoc* 3:419-426.
- Welten MC, de Haan SB, van den Boogert N, Noordermeer JN, Lamers GE, Spaik HP, Meijer AH, Verbeek FJ. 2006. ZebraFISH: fluorescent in situ hybridization protocol and three-dimensional imaging of gene expression patterns. *Zebrafish* 3:465-476.

VI - Supplementary Material

SI Table I - Average Somite Length in micron for the three somite combinations (S3-6, S11-14 and S15-18) and Standard Error of the Mean (SEM).

	Length (um)					
	S3-6	SEM	S11-14	SEM	S15-18	SEM
control	49,4	0,9	36,0	0,9	43,7	2,1
cbr-	66,3	2,2			58,7	2,9
Δ 390			41,4	1,3	33,7	4,0

SII Table II – Average Somite Width in micron for the three somite combinations (S3-6, S11-14 and S15-18) and Standard Error of the Mean (SEM).

	Width (um)					
	S3-6	SEM	S11-14	SEM	S15-18	SEM
control	56,6	1,2	47,2	1,1	45,8	1,5
cbr	107,1	5,3			61,5	2,1
Δ 390			53,3	1,2	50,5	1,6

SIII Table III – Average PSM Width in micron for the control embryos and the Δ 390 treated embryos and Standard Error of the Mean (SEM).

	PSM	
	width	sem
control	45,5	1,2
Δ 390	50,7	1,5

SIV Table IV – Average Somite Height in micron for the three somite combinations (S3-6, S11-14 and S15-18) and Standard Error of the Mean (SEM).

	Somite Height					
	S3-6	SEM	S11-14	SEM	S16-18	SEM
control	93,5	1,7	90	2,3	79,2	3,2
cbr-	98,7	4,4			96,8	2,3
Δ 390			110,9	6,9	155,1	7,1

SV Table V – Average values in μm^3 for the epithelium, somitocoel and total volumes for the combination of somites S16-18.

	S16-18		
	$V_{\text{epithelium}}$	$V_{\text{somitocoel}}$	V_{total}
control	126354,9	5295,1	131649,9
cbr-	277169,3	7154,4	284323
$\Delta 390$	134359,4	2955,3	137314,6

SVI Table VI – Average number of cells per 25 μm of epithelium (medial, rostral and caudal) and 20 μm of somitocoel for the combination of somites S16-18.

	Medial Epithelium			Rostral Epithelium			Caudal Epithelium			Somitocoel		
	S16	S17	S18	S16	S17	S18	S16	S17	S18	S16	S17	S18
control	9,25	10	10,5	8,25	8,5	7,5	8,25	8	7	4,75	6	4,75
cbr-	11,25	10	9	9,25	10,25	9	10	9	8,5	3,5	3,25	4,25
$\Delta 390$	13,25	13,25	11	10	10,25	9,25	10,5	10	9,75	4	3,25	4

SVII Movie S1. Cell movements during somite formation of a $\Delta 390$ electroporated embryo. Notice the occasional loss of cells from the somite epithelium to the blastocoel cavity. The fusion of somites is seen towards the end of the movie. For more details consults Fig. 14.